

ENHANCING GAN LED EFFICIENCY THROUGH NANO-GRATINGS AND
STANDING WAVE ANALYSIS

A Thesis

presented to

the Faculty of California Polytechnic State University,

San Luis Obispo

In Partial Fulfillment

of the Requirements for the Degree

Master of Science in Electrical Engineering

by

Gabriel Michael Halpin

December 2013

© 2013
Gabriel Michael Halpin
ALL RIGHTS RESERVED

COMMITTEE MEMBERSHIP

TITLE: Enhancing GaN LED Efficiency through Nano-Gratings
and Standing Wave Analysis

AUTHOR: Gabriel Michael Halpin

DATE SUBMITTED: December 2013

COMMITTEE CHAIR: Dr. Xiaomin Jin
Associate Professor of Electrical Engineering

COMMITTEE MEMBER: Dr. Dennis Derickson
Department Chair of Electrical Engineering

COMMITTEE MEMBER: Dr. John Sharpe
Associate Professor of Physics

ABSTRACT

Enhancing GaN LED Efficiency through Nano-Gratings

and Standing Wave Analysis

Gabriel Michael Halpin

Improving energy efficient lighting is a necessary step in reducing energy consumption. Lighting currently consumes 17% of all U.S. residential and commercial electricity, but a report from the U.S. Office of Energy Efficiency and Renewable Energy projects that switching to LED lighting over the next 20 years will save 46% of electricity used in lighting. GaN LEDs are used for their efficient conversion of electricity to light, but improving GaN efficiency requires optically engineering the chip to extract more light. Total internal reflection limits GaN LED performance since light must approach the chip surface within 23.6° of normal to escape into air. This thesis systematically studies the effect of index of refraction, material thickness, and nano-grating period on light extraction efficiency. An ITO layer is added to the LED surface to increase the critical angle of light, and standing wave analysis is used to optimize material thicknesses. When these results are combined with the best grating period, light output improves by 254% over the unmodified LED.

ACKNOWLEDGMENTS

Thank you Dr. Jin for introducing me to the field of simulation based LED research. I have enjoyed the challenges of learning a new subject, discovering new things, and learning to read and interpret the data I generated. Your guidance, deadlines, critiques, and experience have been invaluable to me since starting this project.

Dr. Sharpe, thank you for all of the great explanations you gave in class and in office hours. I enjoyed your classes over the last year and know the field better from it.

Dr. Derickson, thanks for fitting my thesis defense into your busy schedule. I appreciate all the time you spend in office hours explaining microwave concepts. We plowed through so much material that quarter.

Mom and Dad, thanks for your support, counsel, encouragement, and the occasional kick in the butt over the last year and throughout my life. I love you.

This project was supported by the NSF Grant IRES Award #1029135 from year 2010 to 2014 and the Chinese National Key Research Lab Collaboration Grant 2012-13, Peking University in China.

TABLE OF CONTENTS

	Page
LIST OF TABLES.....	vi
LIST OF FIGURES.....	viii
ABBREVIATIONS.....	xii
 CHAPTER	
I. INTRODUCTION.....	1
Background.....	2
Health concerns of LEDs vs fluorescents.....	8
II. SIMULATION ENVIRONMENT.....	9
III. GRADUATED INDEX OF REFRACTION.....	12
Simulation Model.....	13
Results.....	16
IV. STANDING WAVES.....	18
Simulation Model.....	18
Above the MQW region: varying ITO thickness.....	19
Below the MQW region: varying Sapphire substrate thickness.....	21
Theory.....	25
Conclusion.....	29

V.	TOP ITO NANO-GRATINGS.....	30
	Simulation Model.....	31
	Gratings - Top Light Extraction.....	33
	Gratings - Total Light Extraction.....	36
	Gratings and Substrate Variation.....	40
	Grating output at different wavelengths.....	44
	Explaining the grating results.....	47
VI.	CONCLUSION.....	49
VII.	FUTURE WORK.....	50
	PUBLICATIONS.....	52
	REFERENCES.....	53
	APPENDICES	
	Appendix A: Finite difference time domain method (FDTD).....	57
	Appendix B: RSoft - Building and Simulating the Model.....	59

LIST OF TABLES

Table	Page
1. LED material thickness and refractive indices at $\lambda = 460\text{nm}$	14
2. Light extracted from the 4 cases in Figure 8.....	16
3. Percent improvement by ITO case (a) over the reference cases at three different thicknesses.....	17
4. Light output intensities at best, worst, and neutral ITO thicknesses.....	21
5. Maxima, minima, and average values from Figure 11.....	25
6. Material thickness required to add an intensity peak and trough.....	26
7. Best and worst top light outputs for the grating at three critical ITO thicknesses with Ref. 1 and 2.....	35
8. Percent improvement of grating on each ITO thickness over Reference 1 and 2.	35
9. Light extraction minima and maxima for the LED with gratings on differing sapphire substrate thicknesses. ITO = 78nm.....	43
10. Percent improvement of top light emission by grating at top light extraction maxima for different sapphire substrate thicknesses and top emission efficiency as % of total emission at top emission maxima. ITO = 78nm.....	43

LIST OF FIGURES

Table	Page
1. Band gaps in materials: direct (left) and indirect (right).....	3
2. The LED junction with an energy level diagram.....	3
3. Two methods of creating white LED light.....	5
4. Critical angle in GaN.....	7
5. Injecting and monitoring light in the LED model.....	10
6. Critical angle of light exiting GaN into Air.....	12
7. LED model shown with ITO grating and Ag reflection layer added.....	13
8. LED models with: a) ITO case, b) Reference 1 - GaN added to make light travel the same number of wavelengths in the LED as experienced in (a), c) Reference 2 - added GaN height = ITO height, d) Reference 3 - unaltered or unconventional LED.....	15
9. The LED model used for standing wave analysis.....	18
10. LED top output intensity as ITO thickness varies from 0 to 450nm at 1nm increments.....	20
11. Output intensity as sapphire substrate thickness increases when ITO thickness is: (a) best case - 78nm, (b) worst case - 260nm, and (c) neutral - 46nm.....	23
12. Top and bottom light emission over time under worst standing wave conditions for top light emission.....	27
13. Top and bottom light emission over time under best standing wave conditions for top light emission.....	28

14.	Electromagnetic fields in the LED under worst standing wave conditions for top emission after reaching steady state. ITO = 78nm, Sapphire = 10,032nm.	28
15.	Electromagnetic fields in the LED under best standing wave conditions after reaching steady state. ITO = 78nm, Sapphire = 10,050nm.....	29
16.	Simulation model for grating study. Triangle height = h & width = w.....	31
17.	The grating case and the references used in the study.....	32
18.	Top emission intensity vs. grating period for the ITO triangle grating on best case ITO, 78nm, with Ref. 1, the no grating case (ITO = 78nm), and with Ref. 2, the conventional LED.....	33
19.	Top emission intensity vs. grating period for the ITO triangle grating on worst case ITO, 260nm, with Ref. 1, the no grating case (ITO = 260nm), and with Ref. 2, the conventional LE.....	34
20.	Top emission intensity vs. grating period for the ITO triangle grating on a neutral ITO thickness, 46nm, with Ref. 1, the no grating case (ITO = 46nm), and with Ref. 2, the conventional LED.....	34
21.	Total light intensity vs. grating period on a best case ITO of 78nm with emission intensities for top, bottom, and sides.....	37
22.	Total light intensity vs. grating period on a worst case ITO of 260nm with emission intensities for top, bottom, and sides.....	37
23.	Total light intensity vs. grating period on a neutral case ITO of 46nm with emission intensities for top, bottom, and sides.....	38
24.	Steady state electric field in LED using best grating for top light extraction and best case ITO. Period = 478nm, ITO = 78nm.....	39

25.	Steady state electric field in LED using worst grating for top light extraction and best case ITO. This period also produced the highest bottom light output. Period = 388nm, ITO = 78nm.....	40
26.	Grating total light extraction on three different sapphire substrate thicknesses with ITO = 78nm. a) best standing wave top light extraction, sapphire = 10,050nm, b) best standing wave total light extraction, sapphire = 10,064nm, and worst standing wave top extraction, sapphire = 10,033nm.....	41
27.	Grating total light output when free space wavelength is 450nm.....	44
28.	Grating total light output when free space wavelength is 470nm.....	45
29.	Comparing grating light outputs for three LED wavelengths.....	46
30.	The Yee cell.....	57
31.	Making a grating triangle in CAD.....	60
32.	The array layout generator.....	62
33.	The newly generated triangle array.....	63
34.	The newly generated triangle array at a 1:1 aspect ratio.....	63
35.	Adding the ITO layer underneath the grating array.....	67
36.	Adding the p-GaN layer.....	68
37.	Light bar launch parameters.....	69
38.	The top light monitor.....	70
39.	Left light monitor.....	71
40.	Setting up the simulation time steps and meshing.....	72

ABBREVIATIONS

CAD - computer aided design
EM - electro-magnetic
FDTD - finite difference time domain (analysis)
GaN - Gallium Arsenide
ITO - Indium Tin Oxide
LED - light emitting diode
MQW - multi quantum well (light emitting region of LED)

CHAPTER 1: INTRODUCTION

Over the last 60 years, the US annual electricity consumption has increased by 1300% to 3,856 terawatt hours. Lighting, at 17% of all US residential and commercial electrical use, stands out as a significant area to reduce energy consumption. While the reasons to reduce energy use vary from government objectives, like achieving energy independence, to corporations who seek larger profit margins and reduced environmental footprints, reducing the consumption of electricity through more efficient lighting is desired. A report [1] from the U.S. Office of Energy Efficiency and Renewable Energy projects that switching to LED lighting over the next 20 years will save 46% of electricity used in lighting.

Gallium nitride (GaN) LEDs are an important component in the switch to solid state lighting since they convert electricity efficiently into light and continue to increase in efficiency every year. While residential incandescent light bulbs have plateaued at 13 lumens per watt (lm/W) [1], commercial LEDs worked at 70 lm/W in 2010 and by early 2103, lab efficiencies reached 276 lm/W [2]. This thesis seeks to improve GaN LED light output by increasing light extraction efficiency from the chip.

Background

The wavelength or color of an LED depends on the energy band gap, E_g , of the semiconducting material used. Semiconductors with a higher band gap energy like GaN emit in the blue end of the spectrum while lower band gap semiconductors emit in the red or infrared spectrum. Equation 1.1 shows the relationship between bandgap energy and the emitted wavelength where h is Plank's constant, c is the speed of light in a vacuum, and E_g is the band gap energy of the semiconductor [3].

$$\lambda = \frac{hc}{E_g} = \frac{1240}{E_g} nm \quad (1.1)$$

Light emitting diodes are created using direct band gap semiconductors like GaN because they are much more efficient at emitting light than an indirect bandgap semiconductor. In a direct bandgap semiconductor, electrons can easily decay from the conduction band to fill holes in the valence band [4]. As the electrons jump into the lower energy valence band, they shed the excess energy (equal to the band gap energy) in a photon, see Figure 1. Indirect band gap semiconductors like silicon are extremely inefficient light emitters because an electron must absorb lattice vibration energy before it falls into the valence band.

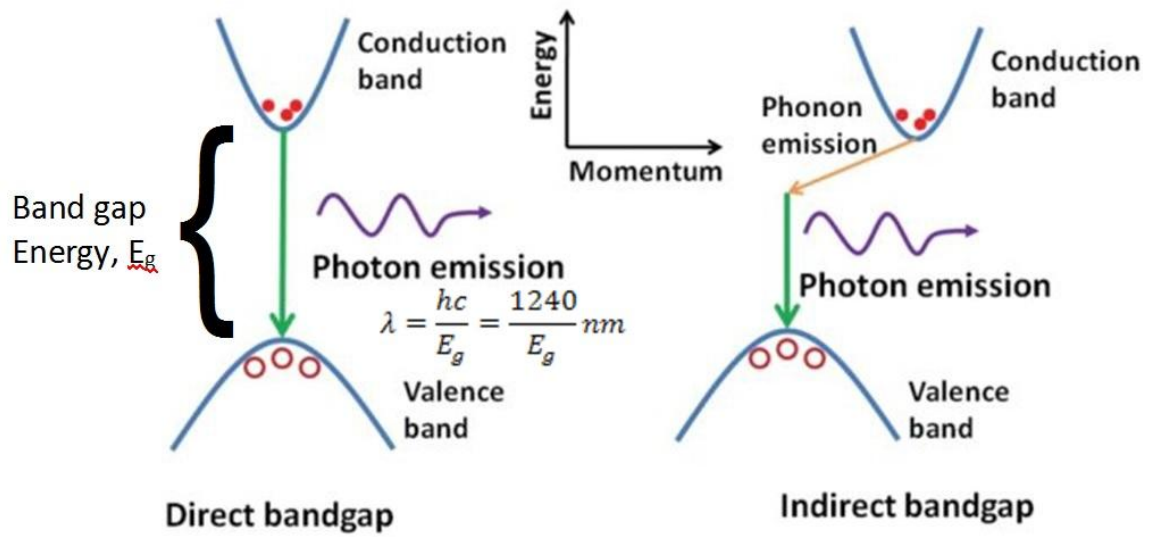


Figure 1 Band gaps in materials: direct (left) and indirect (right).

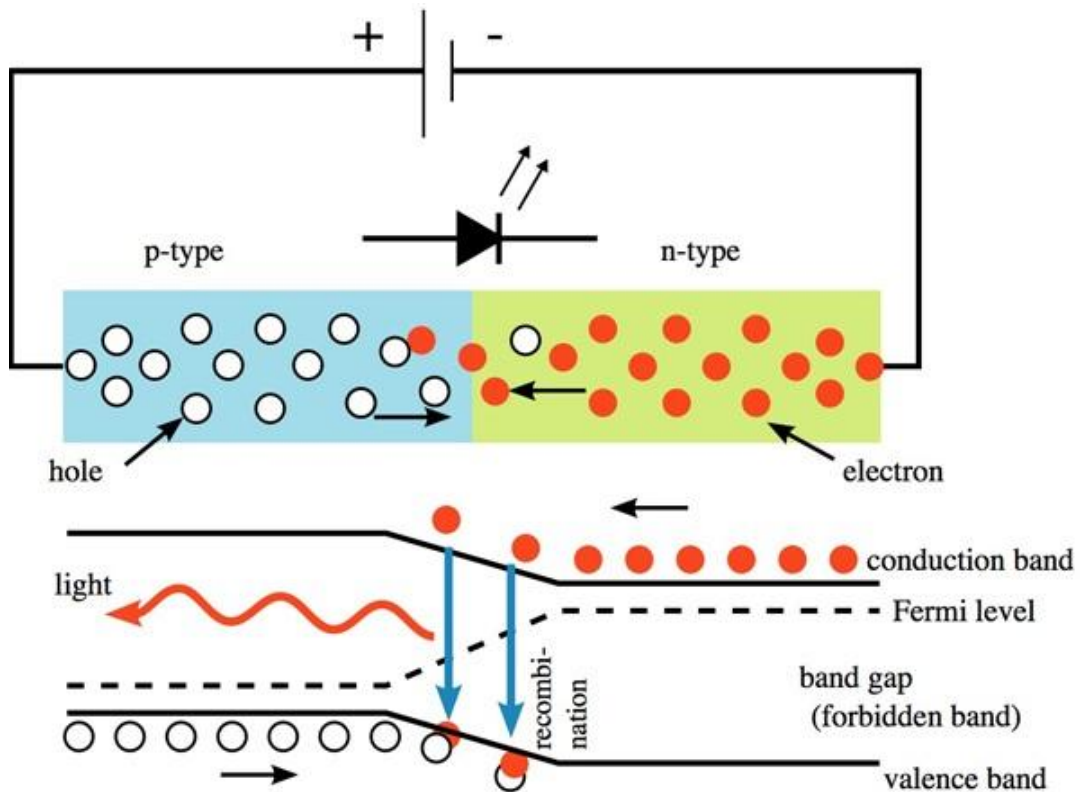


Figure 2 The LED junction with an energy level diagram.

Figure 2 also shows electron hole recombination, but in the diode configuration. The excess electrons on the n-doped side of the junction are pulled to the left by the electric field induced by the battery in the same way that the excess holes in the p-doped region travel to the right. At the p-n junction, the electrons recombine with the holes to reduce their electromagnetic potential and release the excess energy (defined by the band gap), as a photon of light.

There are two methods for creating white light LED. The first combines light from red, green, and blue (RGB) LEDs to create light that the human eye perceives as white. The second uses a blue LED coated with a yellow phosphor to create light with the same color rendering index as the RGB LED, see Figure 3 [5]. The phosphors on the LED absorb some of the blue light created by the LED and re-emit the energy as longer wavelength light broadly centered on yellow. Combining the yellow photons emitted by the phosphor with the blue photons produces a blend of light that our eyes perceive as white.

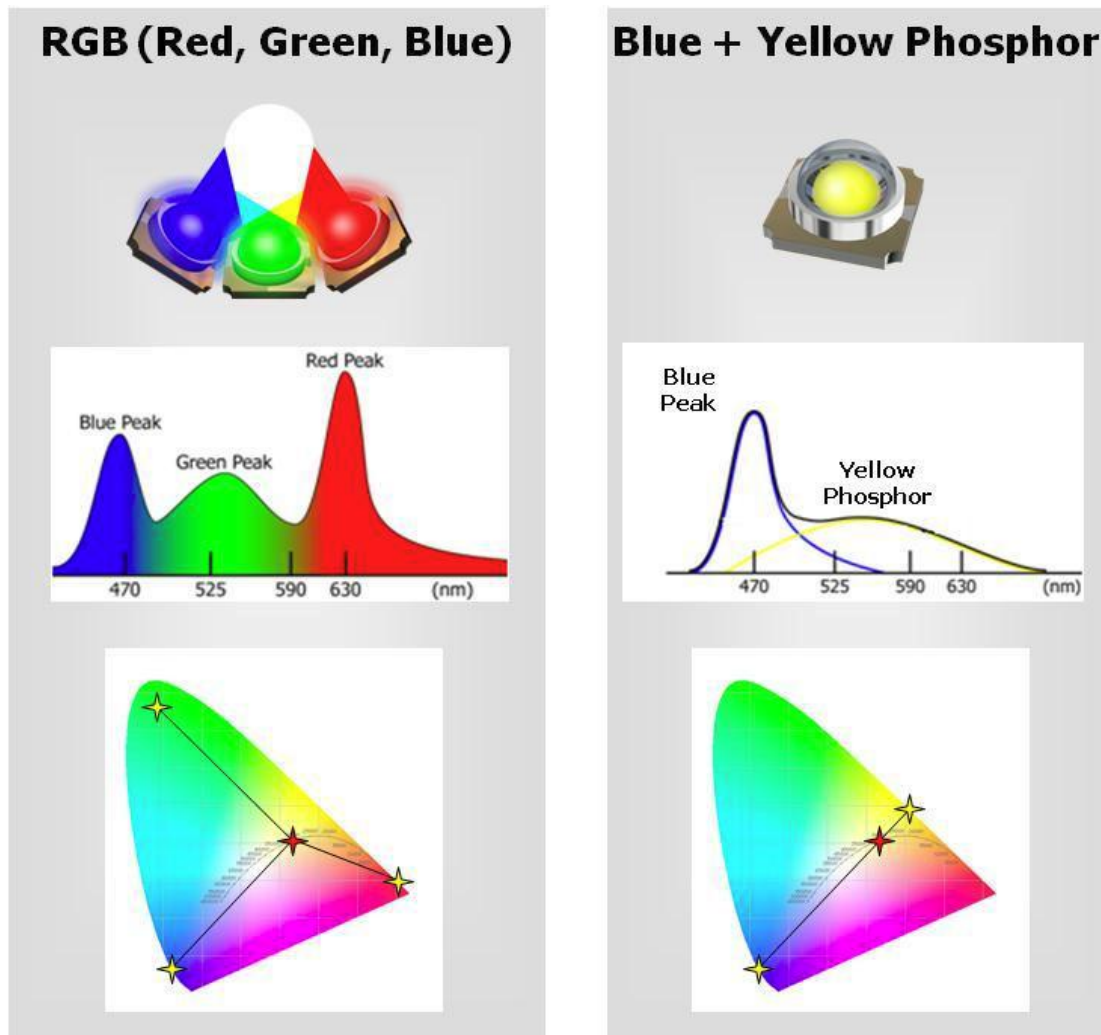


Figure 3 Two methods of creating white LED light.

RGB LEDs have two main disadvantages over the phosphor based LEDs. The first, the three voltage supply circuits are required to drive the LED chips in each RGB unit because each color uses a different voltage. Since the LED driver circuit is the greatest cause of failure in LED bulbs, using three different circuits significantly increases the odds of failure. Once one driving circuit dies, the light output is no longer white but will be a combination of the two remaining colors. Second, as the LED ages, the color will shift since the intensity of the three LEDs will decay at different rates over time.

Phosphor base white LEDs will also color shift towards blue over time as the yellow phosphor ages. However, these LEDs can stay on for such a long time that the color shift is barely perceptible. If multiple phosphors are used to achieve a higher color rendering index [6], a measure of how well lights render color, the color shift due to uneven phosphor decay rate can cause the same color shifting issues that the RGB LEDs can experience.

There are two main areas that can improve the quality and intensity of white light produced in this manner: the phosphors [7] and the blue LED itself. Improving the brightness and efficiency of a GaN LED falls into two categories, the first is improving the quantum efficiency of the LED junction in producing light. The second is the focus of this thesis, improving the optical efficiency of the LED in extracting the light from the diode junction into the surrounding environment.

Improving the light extraction efficiency of GaN LEDs has been approached several different ways. In general, the efficiency of a LED is limited by the maximum angle that light can escape from the surface as defined by Snell's law. Since GaN has a high index of refraction compared to air, light can only escape the LED if it approaches the surface within $\pm 23^\circ$ of normal, as seen in Figure 4.

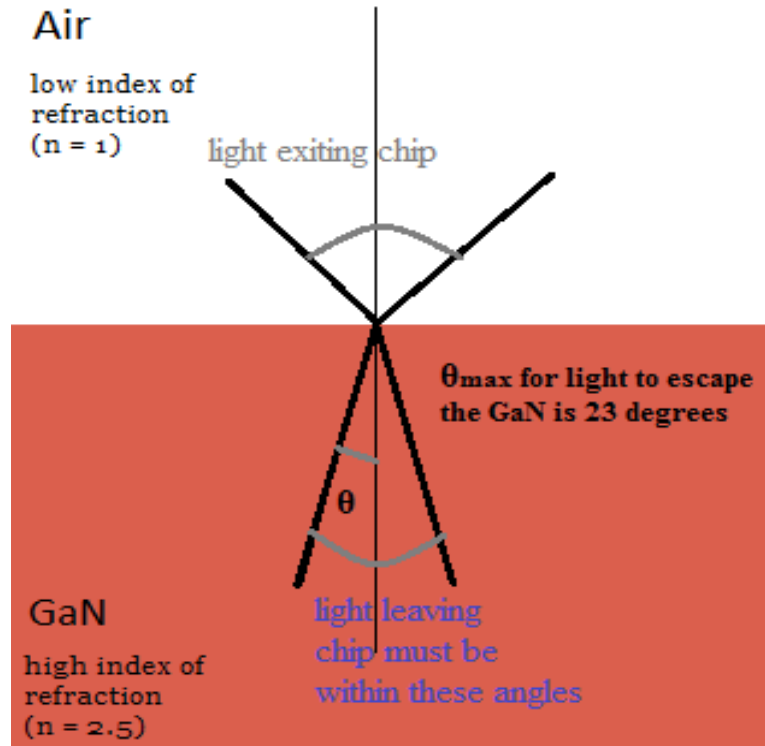


Figure 4 Critical angle in GaN.

Adding a material with an index of refraction between the indices of GaN and air to the LED surface increases the limiting angle [9-14]. Recently, several research groups have used gratings as a method for increasing light output and placed these gratings either on the surface [8-9][13-16], bottom [8][11], or sides [17] of the LED. But most publications on transmission gratings are either focused on micro-grating simulation [8] or are experiments in the micro-grating [10-14][17] or nano-grating [13-16] ranges.

Health concerns of LEDs vs fluorescents

Once manufactured, LEDs pose little health risk to people during their operating life because the chip is encased in epoxy and does not shatter under impact. Unlike fluorescent lights, dropping an LED light will not release mercury vapor or toxins into the environment. However, the LED manufacturing process requires hazardous materials and complex processing and at disposal the LED must be treated as hazardous e-waste since it can leach environmentally toxic metals if deposited in a landfill [18-19].

CHAPTER 2: SIMULATION ENVIRONMENT

The LED models used in this thesis were built in RSoft's CAD environment and simulated using RSoft's finite difference time domain (FDTD) software, Fullwave.

FDTD solves Maxwell's equations on a point by point basis and can accurately simulate the effects of nano-gratings in the LED, such as reflection due to linear dispersion or total internal reflection, transmission of escaping light from the LED, and scattering at the grating. Since FDTD decomposes space and time into separate components, the model is meshed into small cells whose side length must be much smaller than the wavelength of light to obtain accurate results. For more information on the simulation technique see Appendix A: Finite difference time domain method (FDTD).

Knowing how the software injects light into the model and measures escaping light is useful when interpreting the results in the following sections. Light is generated in the multiple quantum well (MQW) region between the positive and negatively doped GaN regions of the diode. Since the computer model simulates light propagation in the LED, we assign all light to emerge as a continuous wave (CW) from the middle of the MQW region as seen in Figure 5. Simulating an entire LED requires more computational power than we have access to, so the model is built as a 2D representative section of the whole LED and implements a uniform light distribution across the MQW region. For more details on how models are build and how simulations are set up, see Appendix B: RSoft: Building and Simulating the Model.

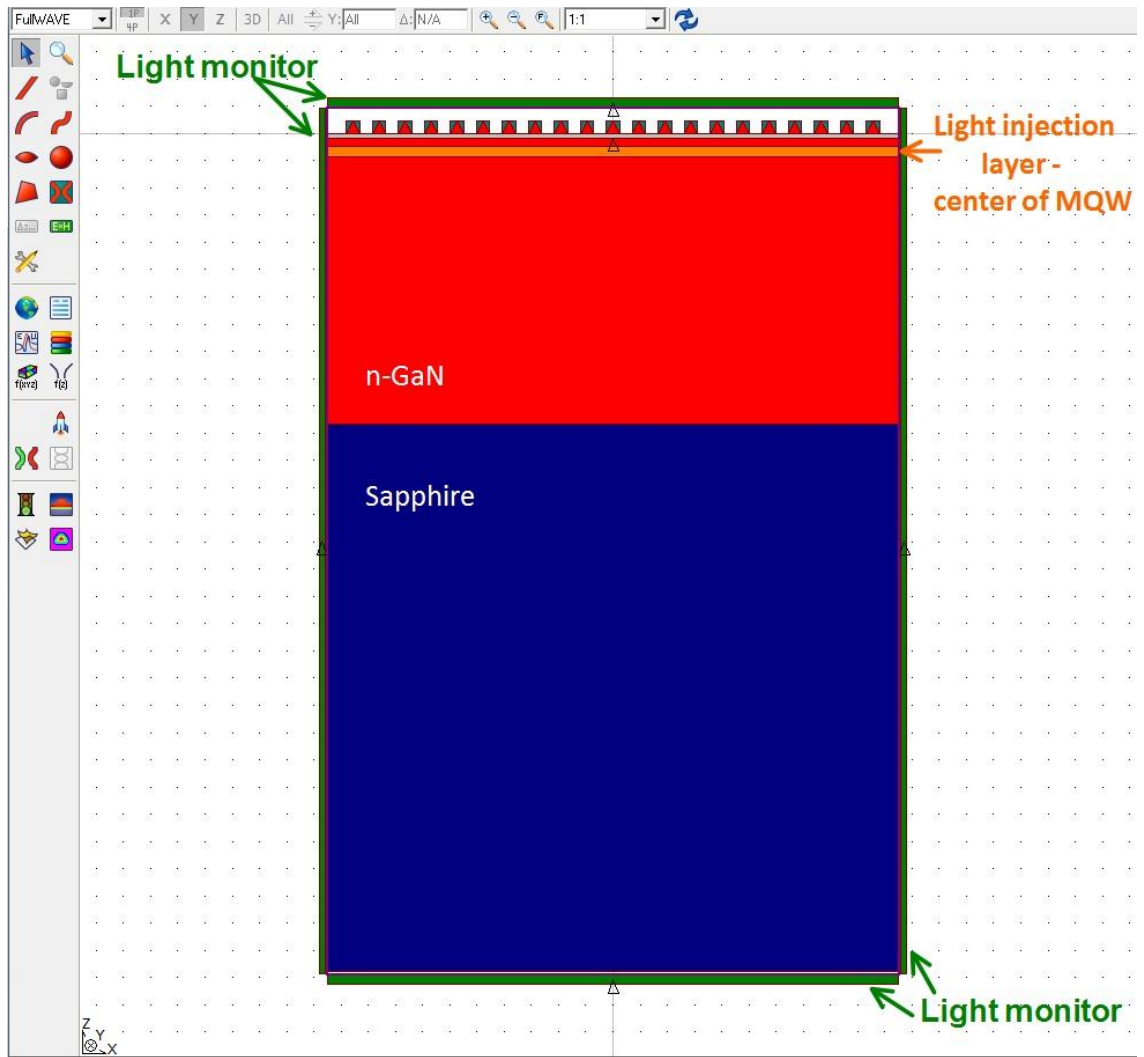


Figure 5 Injecting and monitoring light in the LED model.

The four green bars around the edge of the LED in Figure 5 are the light monitors. They measure the intensity of light emerging from top, bottom, and sides of the LED. The top monitor always sits 560nm above the top non-grating layer of the LED, 100nm higher than the tallest grating triangles. The bottom and side monitors sit 100nm from the LED body. These positions are held constant throughout this research to make sure that the each set of simulations has only one variable that can change the intensity of the light emitted from the LED.

CHAPTER 3: GRADUATED INDEX OF REFRACTION

The efficiency of GaN is intrinsically limited by the maximum angle at which light can escape from the surface of the LED. Snell's law states that the critical angle, the maximum angle at which light can leave one medium and enter another, depends on the materials indices of refraction as seen in equation 3.1.

$$\theta_c = \sin^{-1} \left(\frac{n_2}{n_1} \right) \quad (3.1)$$

This means that light approaching the material interface below the critical angle lies within an escape triangle of allowed angles. From Figure 6, we see that the maximum angle that light can exit the GaN chip and enter air is 23 degrees.

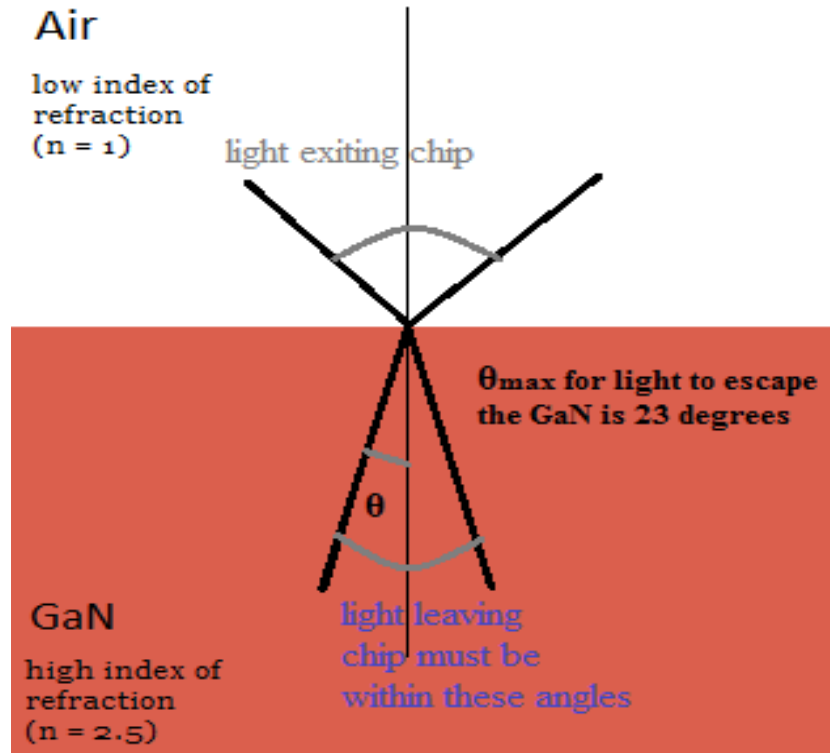


Figure 6 Critical angle of light exiting GaN into Air.

However, if a material of intermediate index of refraction is added between the GaN and air, the critical angle will increase. Section 3 tests the hypothesis that increasing the critical angle will increase light extraction from the LED.

Simulation Model

The LED model, Figure 7, consists of an ITO top grating, p-GaN layer, InGaN/GaN MQW, n-GaN layer, sapphire substrate, and an Ag reflection layer whose thicknesses and refractive indices are listed in Table 1. This model was developed by Peking University's Department of Physics and we have used it at Cal Poly as part of the our collaborative research. The simulations investigating index of refraction differ from Figure 7 by not using the ITO top grating or the reflection layer shown. The sapphire substrate thickness is reduced to 10 μ m to reduce simulation time.

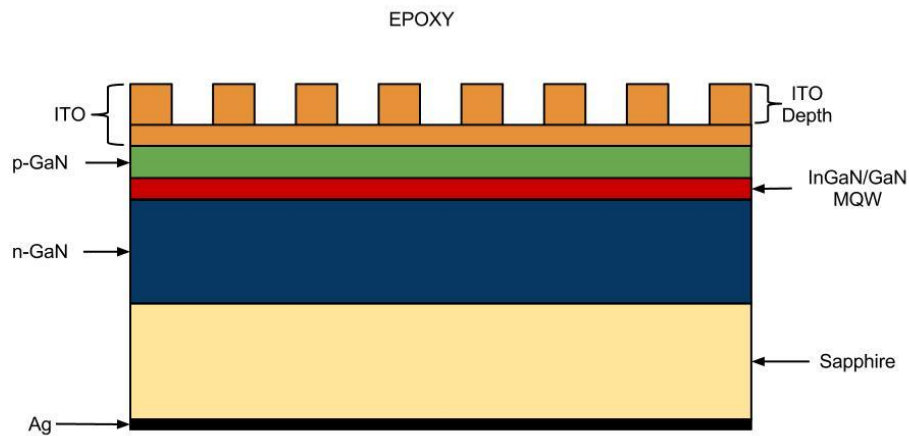


Figure 7 LED model shown with ITO grating and Ag reflection layer added.

Table 1 LED material thickness and refractive indices at $\lambda = 460\text{nm}$.

Material	Thickness (μm)	Refractive Index
p-GaN	0.2	2.5
InGaN/GaN MQWs	0.1	2.6
n-GaN	2	2.5
GaN	3	2.5
Sapphire	80	1.78
ITO	0.23	2.1
Ag	Reflection: 90%	

Indium tin oxide (ITO) is a transparent, conducting material used as the top electrode of the LED. Because ITO has index of refraction between GaN and air adding it to the LED surface increases the critical angle in the LED from 23.6° to 28.4° according to Snell's law. The working hypothesis for this section is that increasing critical angle in the GaN LED will increase the light extraction.

Studying index of refraction as a means of increasing light extraction initially began before standing waves were investigated; and the ITO case, Figure 8a), was compared directly to the unaltered case, Figure 8d). After the standing wave study showed that adding material to the LED surface affects the light extraction efficiency, this chapter was redone with the references shown in Figure 8.

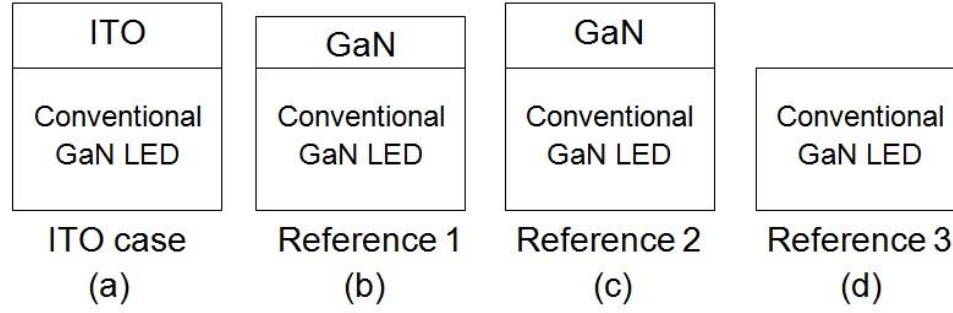


Figure 8 LED models with: a) ITO case, b) Reference 1 - GaN added to make light travel the same number of wavelengths in the LED as experienced in (a), c) Reference 2 - added GaN height = ITO height, d) Reference 3 - unaltered or conventional LED.

Reference 3, the conventional or unaltered LED in Figure 8, is simulated once as a stable reference point. Then the ITO case is simulated at three thicknesses found in section 4, the neutral or thin ITO case of 46nm, the best ITO thickness of 78nm, and the worst case ITO thickness of 260nm. Because the standing wave section shows that the thickness of the ITO affects the light output, light must travel the same distance in the GaN reference case as in the ITO case to cancel out the effects of the standing waves. Reference 2, Figure 8(c), attempts to accomplish this by increasing the GaN thickness above the MQW region by the thickness of the added ITO in Figure 8(a). Since wavelength of light in GaN is different than in ITO according to Eq. 3.2, the final and most accurate model, reference 1, increases GaN thickness above the MQW region to make light travel as many wavelengths between the surface and the MQW layer in it as the light travels in the ITO covered LED. Equation 3.2 states that the wavelength in a material equals the free-space wavelength divided by the material index of refraction at that wavelength.

$$\lambda = \frac{\lambda_0}{n(\lambda)} \quad (3.2)$$

The refractive indices listed in Table 1 are already specified for our operating wavelength of $\lambda_0 = 460\text{nm}$, so the wavelength in ITO is 219nm, and the wavelength in GaN is 184nm. To convert the ITO height in wavelengths to an equivalent number of wavelengths of GaN, divide the ITO height by 219nm per wavelength and multiply by the wavelength in GaN. This gives the equivalent GaN heights for reference 1 as: 38.65nm, 65.53nm, and 218.45nm.

Results

Table 2 Light extracted from the 4 cases in Figure 8.

Light Extracted (a.u.) - ITO case (a)				
ITO height	Top	Bottom	Sides	Total
46nm	1.1491	0.3897	0.1405	1.6793
78nm	1.2604	0.0593	0.0452	1.3649
260nm	0.9963	0.4641	0.2042	1.6645

Light Extracted (a.u.) - Reference 1 (b)				
GaN height	Top	Bottom	Sides	Total
38.65nm	1.1187	0.3185	0.1206	1.5578
65.53nm	1.0831	0.2701	0.0955	1.4488
218.45nm	1.0808	0.2679	0.0912	1.4399

Light Extracted (a.u.) - Reference 2 (c)				
GaN height	Top	Bottom	Sides	Total
46nm	1.1146	0.2942	0.1105	1.5193
78nm	1.1679	0.2805	0.0954	1.5439
260nm	1.2851	0.2842	0.1099	1.6792

Light Extracted (a.u.) - Reference 3 (d)			
Top	Bottom	Sides	Total
1.1548	0.22684	0.069342	1.4510

Table 3 Percent improvement by ITO case (a) over the reference cases at three different thicknesses.

ITO height	% improvement in top light extraction by ITO over:		
	Ref. 1	Ref. 2	Ref. 3
46nm	2.72	3.10	-0.49
78nm	16.37	7.92	9.14
260nm	-7.82	-22.47	-13.73

Table 3's results show that the ITO case usually improves light extraction when compared against the most accurate reference model - reference 1. But adding a material interface between the MQW and the top of the LED changes the light output more than a simple change in index of refraction should account for. If the change in refractive index was isolated from the standing wave results, the light output should either remain unchanged or show a uniform increase in light extraction resulting from the increase in light extraction angle.

As seen in the next section, standing waves exist throughout the LED and affect light output. Adding the ITO interface introduces an interface for internal reflection to occur at and changes the steady state standing wave pattern inside the LED. While we determine from this study that increasing the critical angle does increase light output, the extent that light output improves is complicated by standing wave interference.

CHAPTER 4: STANDING WAVES

Standing waves in an LED can either increase or decrease light output from an LED by constructively or destructively interfering at the top surface. By changing the thicknesses of the ITO and sapphire layers, we show that standing wave interference patterns exist in the LED. Studying this effect shows how much the standing wave pattern can either increase or decrease the light extraction from a chip and is an important step in forming a complete light optimization study of a GaN LED.

Simulation Model

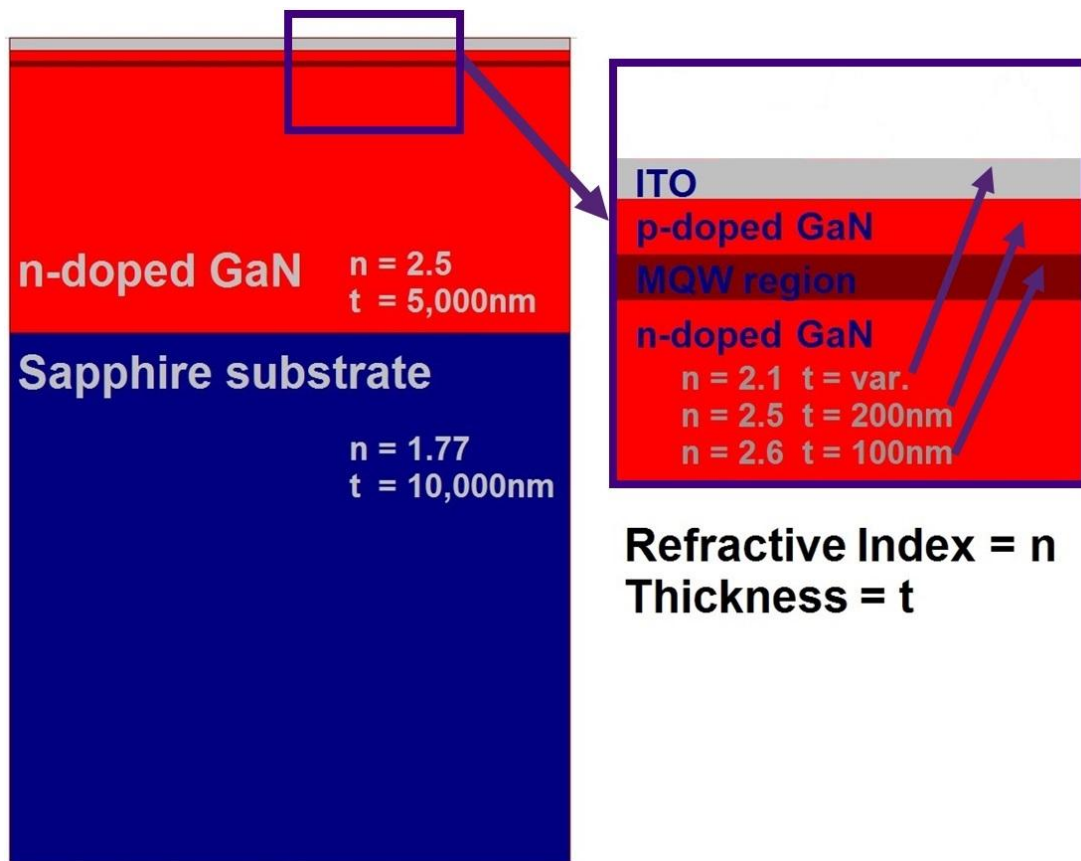


Figure 9 The LED model used for standing wave analysis.

Above the MQW region: varying ITO thickness

The variation in light output during the initial index of refraction study (Section 3) started the investigation of standing waves. I noticed that changing the ITO thickness changed the light output intensity on my simulations. Also Greg Chavoor's thesis data [22] showed that changing the sapphire substrate thickness changed the top light intensity. From these observations, we hypothesized that standing waves must exist inside the LED and could affect light output by either constructively or destructively interfering at the LED to air interface. To prove or disprove this hypothesis, I chose to incrementally add ITO to the surface of the LED. If no standing wave is present, we should observe a linearly decreasing light output as the ITO is added. But, if a standing wave does exist, adding ITO should cause the output to sinusoidally fluctuate with a linear decrease in output intensity.

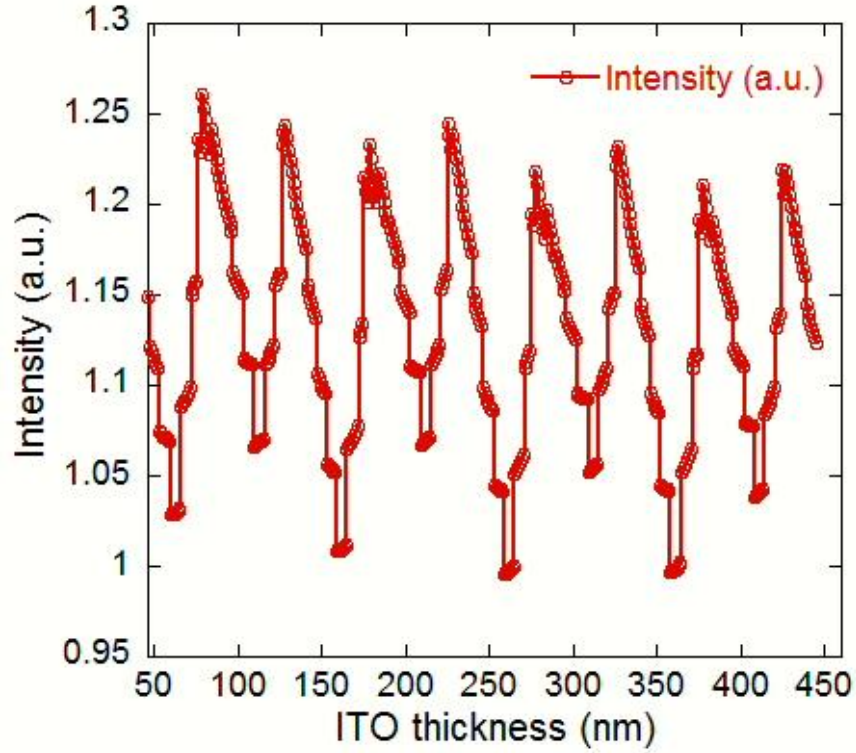


Figure 10 LED top output intensity as ITO thickness varies from 0 to 450nm at 1nm increments.

Figure 10 shows us that as ITO is added, a roughly sinusoidal standing wave pattern emerges whose peak output intensity gradually decreases with increasing material thickness as we expected a standing wave pattern should. We find that the best case ITO thickness occurs at 78nm, the first constructive interference peak, while the worst case ITO occurs at 260nm. As a third reference, 46nm is chosen because its output is the same as the unmodified reference LED. The standing wave period is observed to be 50nm. The results in Table 4 show that the best case light output can increase light extraction by 9.6% and the worst case can decrease light extraction by 13.5%. This gives us a total light increase of 26.7% when the LED thickness changes from worst to best case ITO thickness.

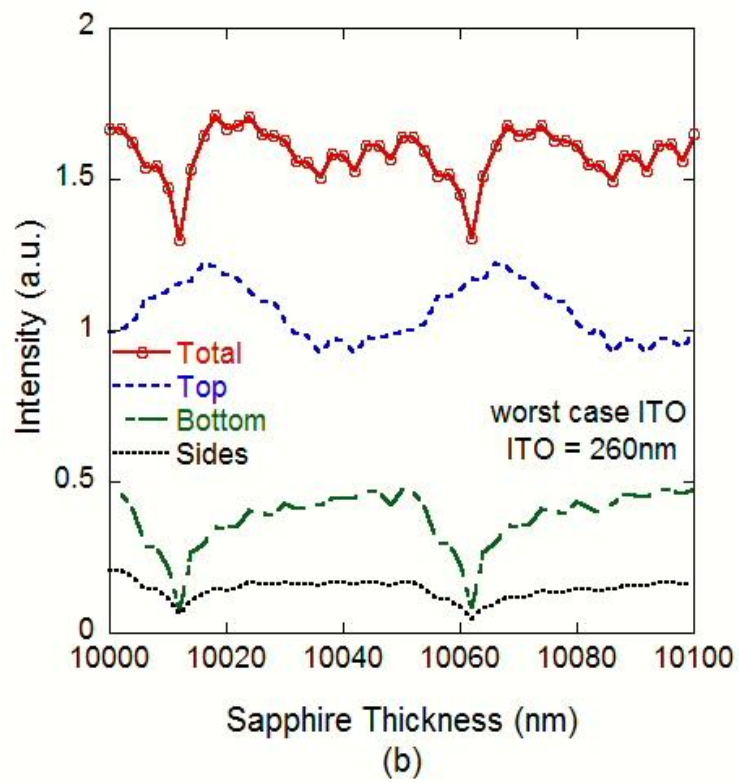
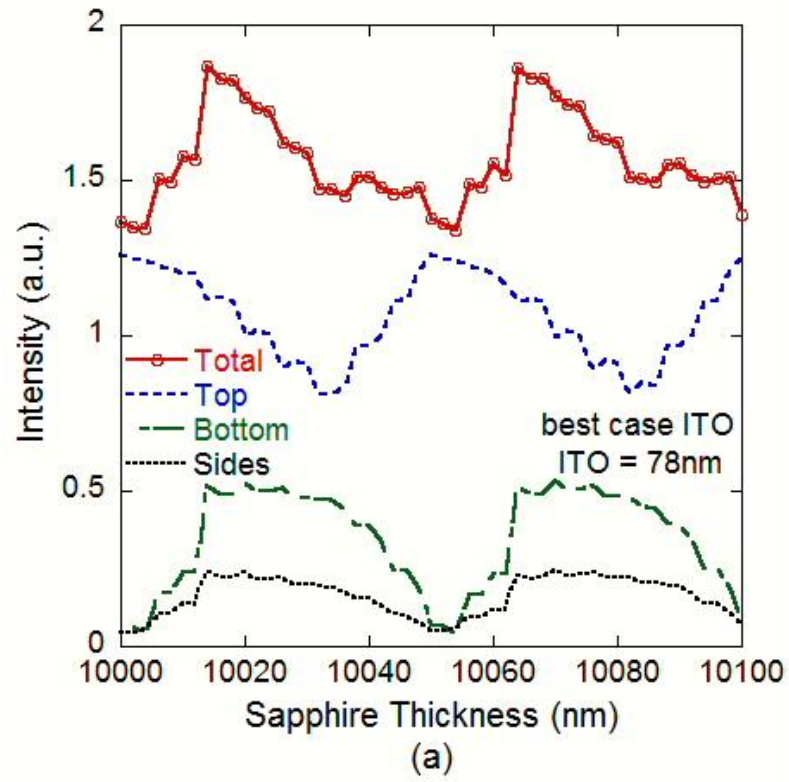
Table 4 Light output intensities at best, worst, and neutral ITO thicknesses.

ITO thickness	Output Intensity (a.u.)	% improvement over Ref. 3 (Figure 8)
78nm	1.2606	9.617
260nm	0.9946	-13.513
46nm	1.1500	0.000

This section shows that a standing wave does exist in the LED and can significantly affect the output intensity of the LED.

Below the MQW region: varying Sapphire substrate thickness

Varying the ITO thickness in section 4.2 showed that the thickness of the region above the MQW is an important aspect controlling light output intensity. The next logical step then is determining if the device thickness below the MQW region effects light output. If it does effect output, we then must determine how much thickness can change the output. To investigate, I increased the sapphire substrate thickness from 10,000nm, the thickness used in section 4.2, up to 10,100nm in steps of 2nm. The simulations were run three times, once for each ITO case found at the end of section 4.2: a best case ITO of 78nm, a worst case ITO of 260nm, and a neutral case ITO of 46nm. During these simulations, four light monitors are used to collect the light emitted from the top, bottom, and sides because additional monitors allow us to form a more complete picture of light distribution exiting the LED.



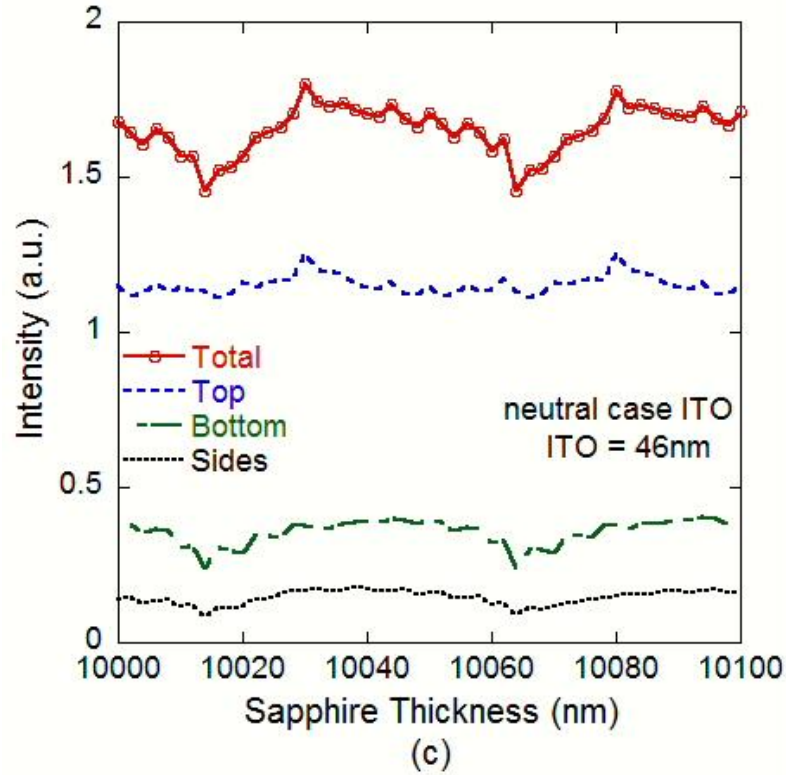


Figure 11 Output intensity as sapphire substrate thickness increases when ITO thickness is: (a) best case - 78nm, (b) worst case - 260nm, and (c) neutral - 46nm.

The results in Figure 11 show that increasing sapphire substrate thickness does modify the standing wave pattern at the three ITO thicknesses. They also show that the LED successfully emits more of its light out the top than the bottom or sides. This is important because top light emission is the preferred direction for light to exit the chip. The bottom usually has an opaque electrical contact attached and a significant portion of light travelling horizontally through the LED will be absorbed before exiting the LED side wall. Figure 11 also shows that modifying the ITO and sapphire substrate thicknesses can selectively increase top light emission while simultaneously reducing side and bottom light emission. However, total light emission is minimized in Figure 11(a) when top emission reaches its peak value because bottom and side emission approach zero at that point. The total light maxima occurs when top light emission is

above average and bottom and side emissions regain their maximum output. Figure 11(a) shows that increasing sapphire substrate thickness reduces the best case ITO light extraction from 1.26 a.u. to 0.81 a.u. It also shows that the best case ITO thickness provides favorable conditions for large standing wave oscillations. If the sapphire substrate thickness can be fabricated within a ± 5 nm tolerance, the 78 nm ITO thickness provides the highest top light extraction of our three cases and should be used with a 10,050 nm sapphire substrate thickness when fabricating GaN LEDs. The largest total light extraction, 1.87 a.u. at a sapphire substrate thickness of 10,014 nm also provides the potential for achieving higher top light extraction if a reflective layer is added to the bottom of the substrate.

From Figure 11(b), the worst case ITO, we observe that as substrate thickness increases, light output increases to 1.22 a.u. from a minimum of 0.92 a.u. While this case does not have the same intensity of minima and maxima that occurs with the best case ITO thickness, their average top and total light extraction values are very similar as seen in Table 5. This averaging out occurs because the worst case ITO has a higher total light extraction for more thicknesses, but around peak the best case ITO has significantly higher total light output. The results show that as the sapphire substrate thickness is changed, the standing wave conditions in the LED are modified. For the best case ITO thickness, adding sapphire reduced the top light output, but for the worst case ITO thickness, adding sapphire increased the top light output.

The neutral case ITO thickness of 46 nm is remarkable for its almost constant top light output as sapphire thickness increases. From the previous two cases, we would expect that the neutral case would display a standing wave pattern that is a mean of the

best and worst. Instead, Figure 11(c) shows that the 46nm ITO thickness almost completely removed any variability caused by differences in sapphire substrate thickness. Also, its average top and total light outputs are 91.3% and 88.5% of the best outputs shown in Table 5, higher than the averages of either the best or worst case ITO. Therefore if variation in sapphire substrate thickness occurs during the fabrication process, a 46nm top ITO coating should be used to provide the highest light output with the least variation.

Table 5 Maxima, minima, and average values from Figure 11.

		Sides	Bottom	Top	Total
Best case ITO, 78nm	Maximum:	0.24201	0.53394	1.26040	1.86837
	Minimum:	0.04450	0.03962	0.80891	1.34119
	Average:	0.16055	0.34142	1.06470	1.56667
Worst case ITO, 260nm	Maximum:	0.20698	0.47998	1.22160	1.71034
	Minimum:	0.04563	0.08030	0.92181	1.29777
	Average:	0.14383	0.38064	1.05930	1.58376
Neutral case ITO, 46nm	Maximum:	0.17633	0.40603	1.25570	1.79937
	Minimum:	0.08369	0.23821	1.11050	1.45522
	Average:	0.14433	0.35646	1.15315	1.65394

Theory

To verify the effect of standing waves on top light extraction, we must compare the computational results against theory. We observe that the ITO standing wave data shows a 50nm period for the top emission intensity, and the sapphire data also observe shows a 50nm period. The free space wavelength, λ_0 , of light used in the experiment is 460nm. We then calculate the wavelength of light in each material using equation 4.1 where n is the material's index of refraction at that wavelength.

$$\lambda = \frac{\lambda_o}{n(\lambda)} \quad (4.1)$$

Adding sapphire increases the distance that the light travels before escaping from the top surface of the LED by twice the added thickness since this light must pass through the added material, reflect, and travel back up to the surface. Also, the average distance traveled above the MQW region is double the added ITO thickness when the direct escape path and a primary reflection are combined.

Table 6 Material thickness required to add an intensity peak and trough.

Material	n	Wavelength, λ , in Mat'l (nm)	ΔL in mat'l for a path length increase of λ (nm)	ΔL req. in mat'l to measure period in light intensity (nm)
ITO	2.1	219.0	109.5	54.8
GaN	2.5	184.0	92.0	46.0
MQW	2.6	176.9	88.5	44.2
Sapphire	1.77	259.9	129.9	65.0

The results in Table 6 show that the calculated results are in the same range as the FDTD generated results. But, this shows that the period of the standing wave measured from the top of the LED is significantly modified by the path length within the GaN and MQW layers to reach a period of 50nm. When the theoretical periods are interpreted with Figure 12, the results lead us to believe that there are reflections occurring at every material interface and that the steady state light output is a combination of all of the different light paths as they emit at the LED surface. By comparing Figure 12 with Figure 13, we see that the worst standing wave case has large reflections within the LED that require a longer simulation window to reach steady state conditions than the best standing wave case does. Note that time is measured in μm , this is a function of how FDTD breaks down the model into time and space components. Time is measured in

units of distance by the software since light covers a specific distance in the material during each discrete time step. The best standing wave conditions reach maximum light output within 20 μm of time steps and the top output is barely changed by returning reflections from the sapphire substrate. Also, the electromagnetic fields in Figure 14 show that worst standing wave thicknesses continue to have strong fields throughout the LED under steady state conditions where the best standing wave conditions, Figure 15, show almost no electromagnetic fields below the MQW region in steady state.

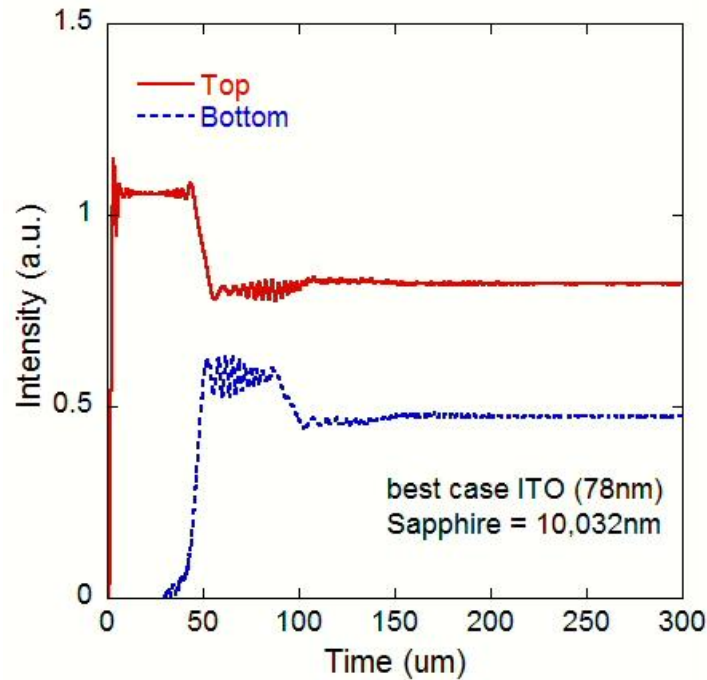


Figure 12 Top and bottom light emission over time under worst standing wave conditions for top light emission.

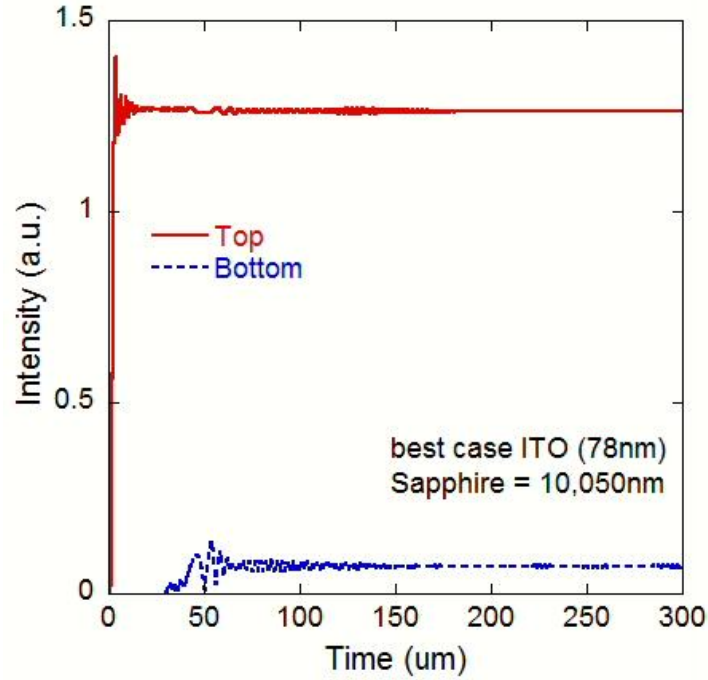


Figure 13 Top and bottom light emission over time under best standing wave conditions for top light emission.

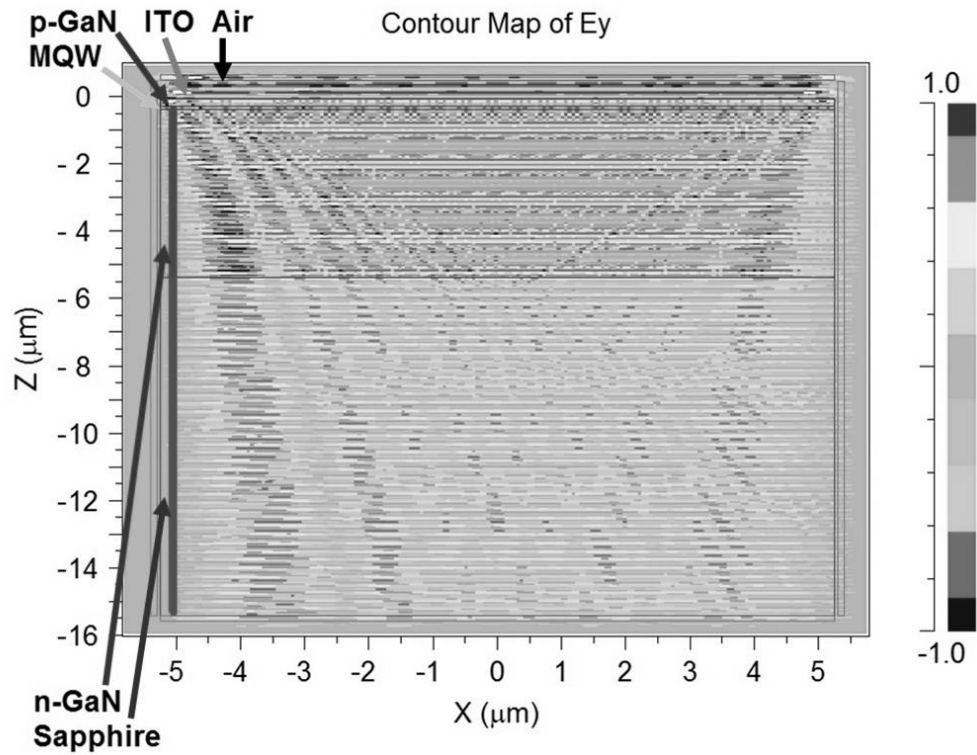


Figure 14 Electromagnetic fields in the LED under worst standing wave conditions for top emission after reaching steady state. ITO = 78nm, Sapphire = 10,032nm

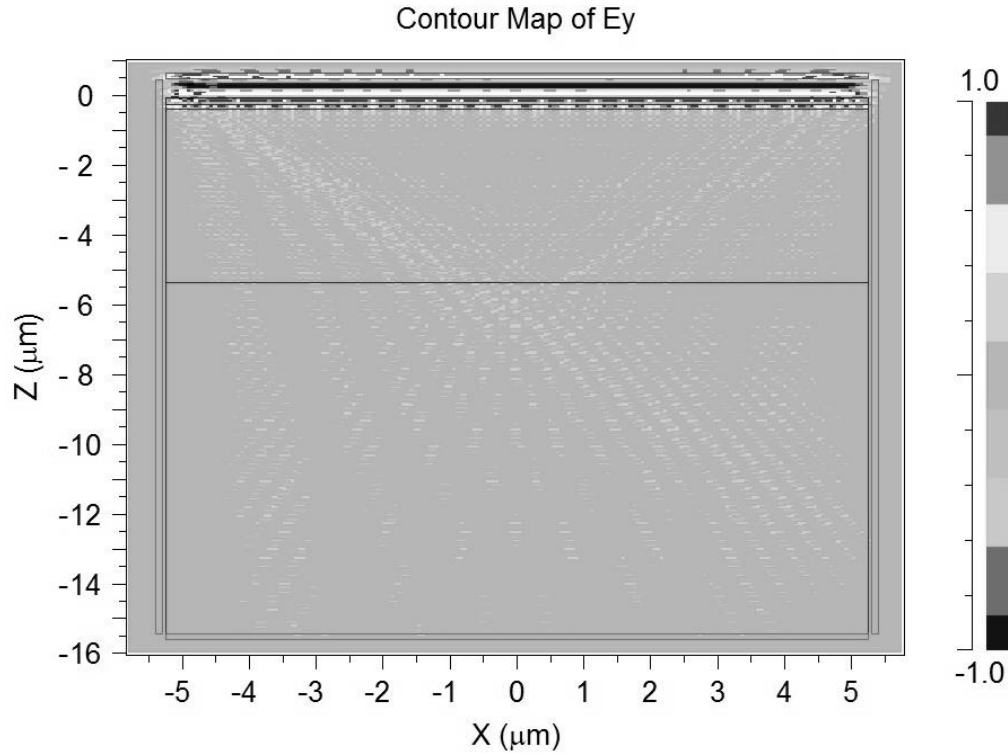


Figure 15 Electromagnetic fields in the LED under best standing wave conditions after reaching steady state. ITO = 78nm, Sapphire = 10,050nm

Conclusion

Standing wave analysis shows that interference patterns exist in the LED and are effected by both ITO and sapphire thicknesses. Through modifying these thicknesses we can cause top light output to range from 0.809 to 1.260 a.u. while the unmodified LED model from Peking University, reference 3, output 1.150 a.u (with a sapphire thickness of 10,000μm). Improving light output from the worst case to best case increases light output by 55.8 and the best case increases light extraction by 9.6% over reference 3.

CHAPTER 5: TOP ITO NANO-GRATINGS

Gratings can improve the light extraction efficiency in GaN LEDs by providing additional angles for light to escape from the surface [20-21] or by providing a region of an intermediate index of refraction at the LED surface. The gratings can be placed on the surface [8-9][13-16], sides [17], or bottom [8][11] of the LED. However, most publications on transmission gratings are either focused on micro-grating simulation [8] or are experiments in the micro-grating [10-14][17] or nano-grating [13-16] ranges. Comprehensive study on ITO nano-gratings with standing wave analysis is still very novel in this field. In this study, nano-scale transmission ITO gratings are systematically studied at sub wavelength periods while considering the effects of standing waves.

Simulation Model

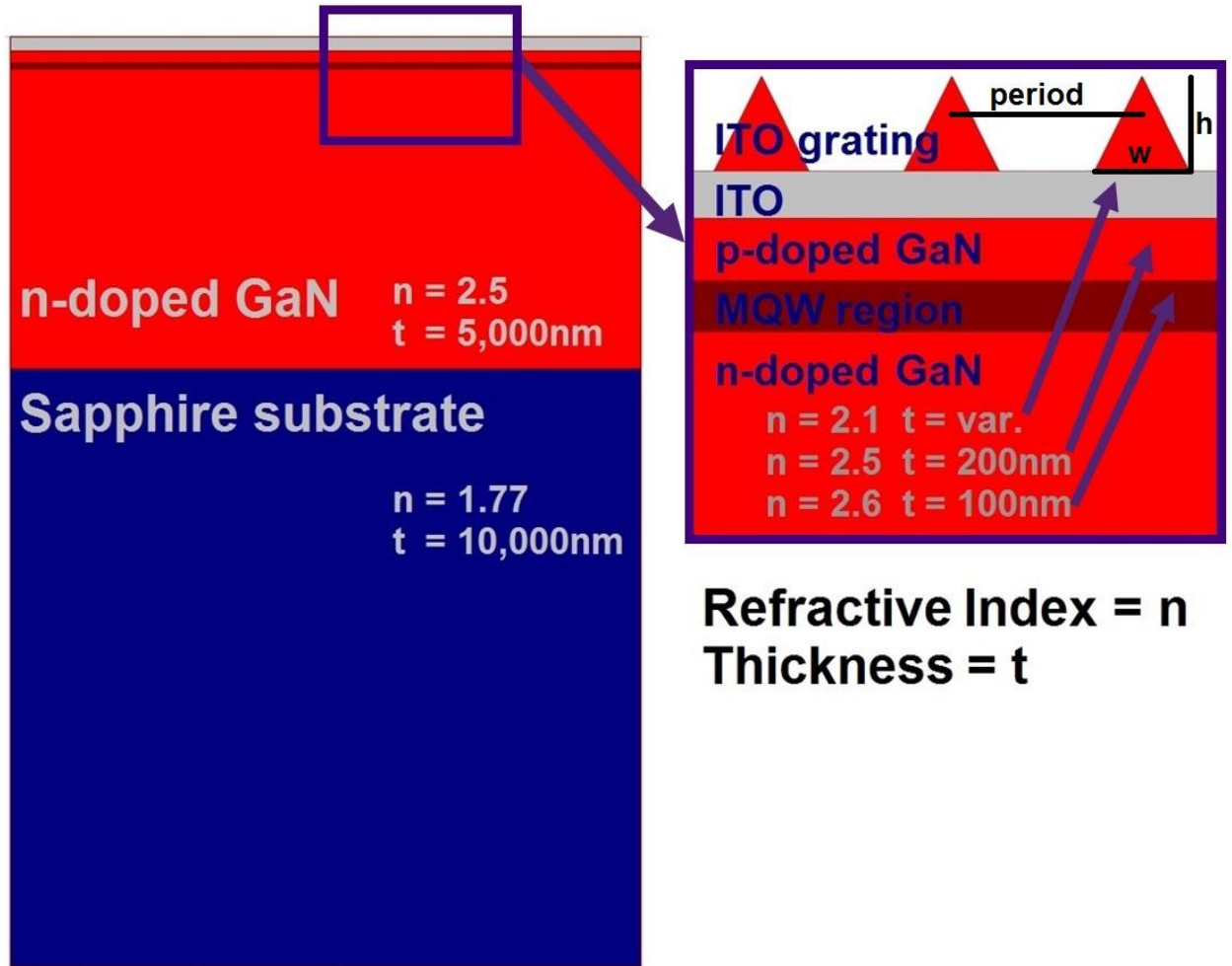


Figure 16 Simulation model for grating study. Triangle height = h & width = w .

Triangle height = h and width = w . The additional angles provided by gratings provide light more angles to escape from. At sub-wavelength periods, nano-scale gratings can be understood as a gradually changing the effective index of refraction between the ITO and the air.

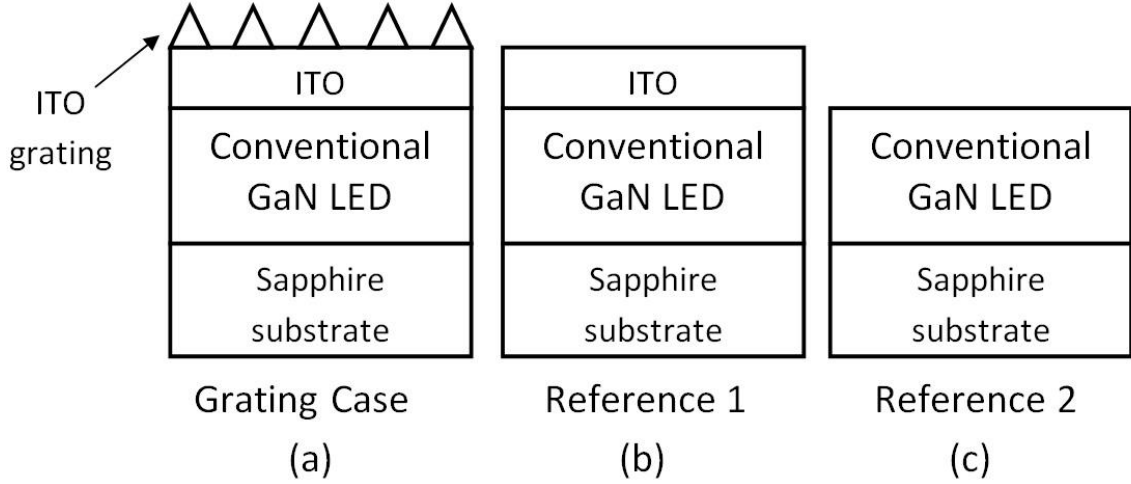


Figure 17 The grating case and the references used in the study.

The grating period used in this study is swept from 92nm to 920nm so we can find the grating period that maximizes top light extraction. I chose this range for the grating because it sweeps the height and width of the triangles in the grating from $\lambda/10$ to λ . The grating fill factor was held at 0.5 and the ratio of triangle height to width was kept at 1 throughout the study to focus on the effect of grating period and standing waves on light output. Because standing wave analysis showed material thicknesses for the ITO and sapphire layer that both maximize and minimize light extraction before gratings are added, we study the grating output at those key thicknesses. As material thicknesses change, the grating output is compared to the instance of reference 1, Figure 17, that has the same material thickness. However, reference 2, the conventional LED, is used as an unchanging reference and its sapphire substrate thickness remains fixed at 10,000nm.

Gratings - Top Light Extraction

The plots in Figure 18 - Figure 20 show the top light emission intensity versus grating period on each ITO thickness and compare the grating output to the light intensity emitted from references 1 and 2.

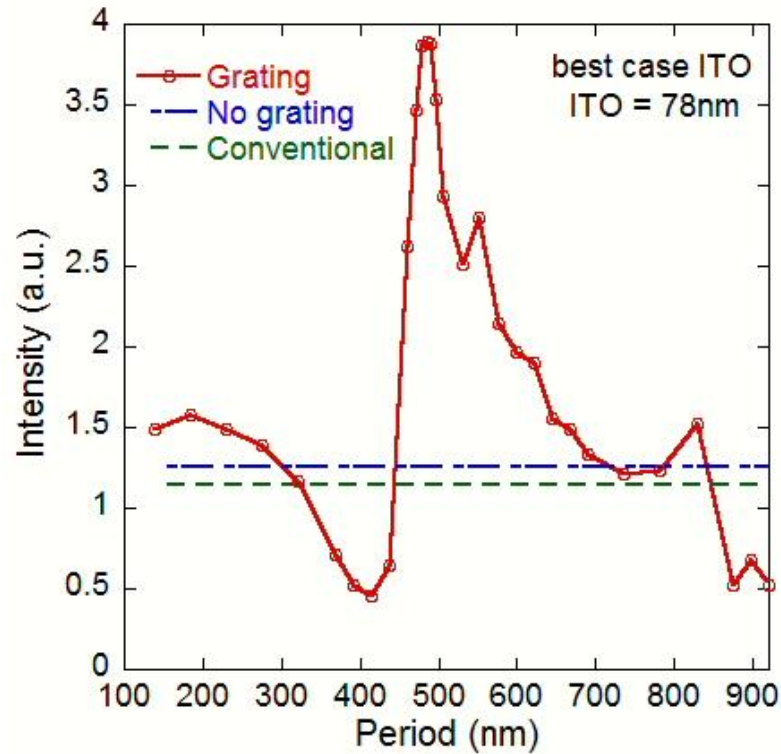


Figure 18 Top emission intensity vs. grating period for the ITO triangle grating on best case ITO, 78nm, with Ref. 1, the no grating case (ITO = 78nm), and with Ref. 2, the convention LED.

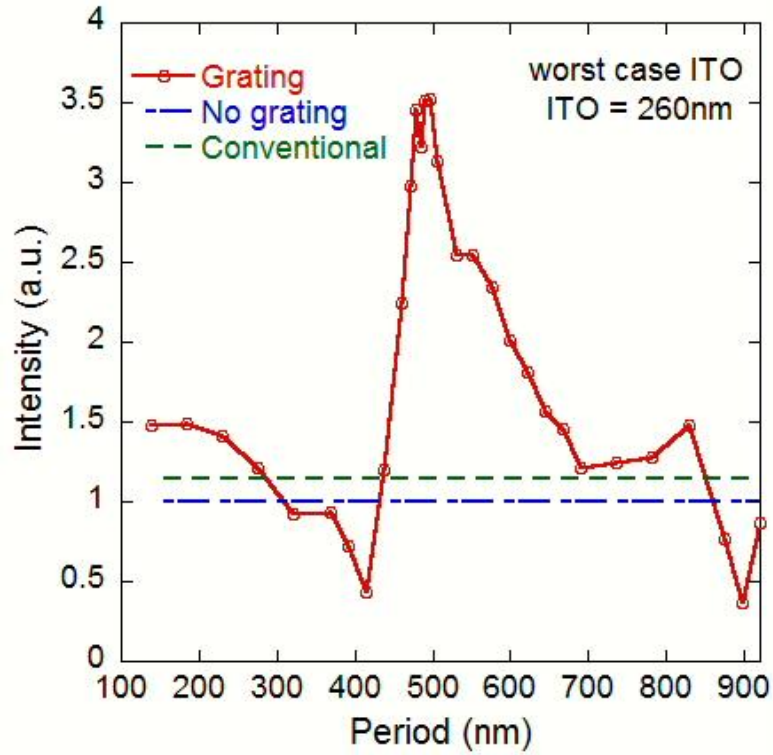


Figure 19 Top emission intensity vs. grating period for the ITO triangle grating on worst case ITO, 260nm, with Ref. 1, the no grating case (ITO = 260nm), and with Ref. 2, the convention LED.

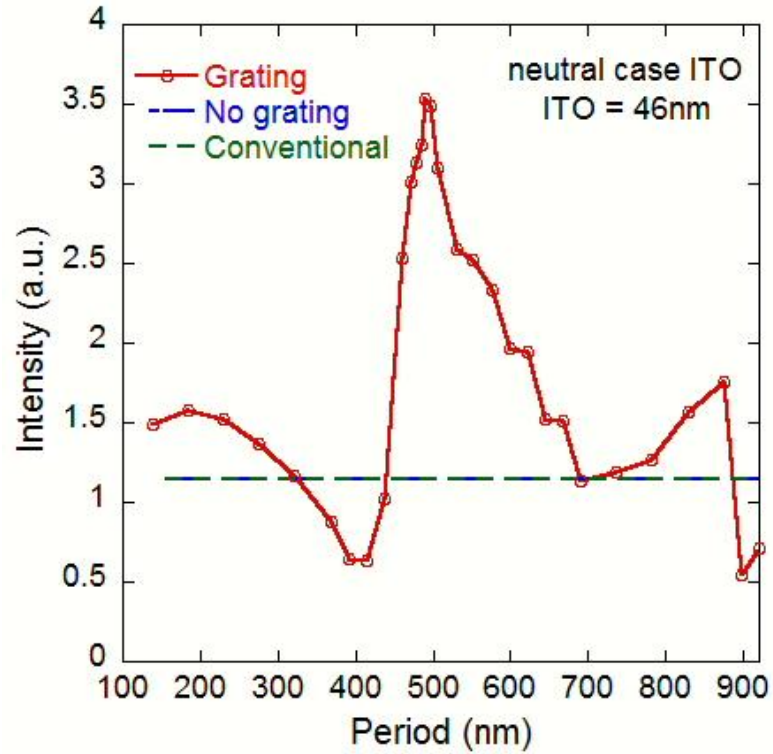


Figure 20 Top emission intensity vs. grating period for the ITO triangle grating on a neutral ITO thickness, 46nm, with Ref. 1, the no grating case (ITO = 46nm), and with Ref. 2, the convention LED.

The graphs of intensity versus grating period in Figure 18 - Figure 20 show that gratings can significantly improve light output around a grating period of 500nm and increase light output at most periods. However, the results also show that the grating can reduce light output by more than 50% if a period of 400 or 900nm is used. As expected, the grating on the best case ITO layer has the highest light output at 3.89 a.u. But the grating unexpectedly extracts almost as much light from worst case ITO as it does from the neutral thickness ITO. Comparing the best and worst grating outputs in Table 7 against reference 1 and 2 shows that the worst grating light extraction does occur with the worst case ITO. But the best case ITO can have a lower output than neutral case ITO when poor grating periods are used.

Table 7 Best and worst top light outputs for the grating at three critical ITO thicknesses with Ref. 1 and 2.

	best case ITO thickness (78nm)	worst case ITO thickness (260nm)	neutral ITO thickness (46nm)
best grating output (a.u.) (@ period = 490/484/496nm)	3.8947	3.5175	3.5393
worst grating output (a.u.) (@ period = 898/414/898nm)	0.45608	0.37002	0.54088
Ref. 1, no grating (a.u.)	1.2604	0.45608	1.1500
Ref. 2, conventional (a.u.)	1.1500	1.1500	1.1500

Table 8 Percent improvement of grating on each ITO thickness over Reference 1 and 2.

	% improvement of grating over ref. when on:		
	best case ITO thickness ITO = 78nm	worst case ITO thickness ITO = 260nm	neutral ITO thickness ITO = 46nm
Reference 1, no grating ITO	209.0	253.1	208.0
Reference 2, the conventional LED	238.7	205.9	207.8

Table 8 shows that the greatest increase in light extraction over reference 2, the conventional LED, occurs when the grating is on best case ITO thickness. This creates a 238.7% increase in top light output. However, the grating's largest relative improvement occurs when the worst case ITO light output increases by 253.1% over reference 2 to nearly equal the grating output of the neutral case ITO.

Gratings - Total Light Extraction

We next looked at the total light emitted from the LED as grating period changes. Understanding where light is emitted is important because some systems are designed to capture and direct light emitted from the sides and bottom of the LED. For these systems, maximizing total light output may be more important than maximizing top light emission if top and total light emission are not maximized at the same grating period.

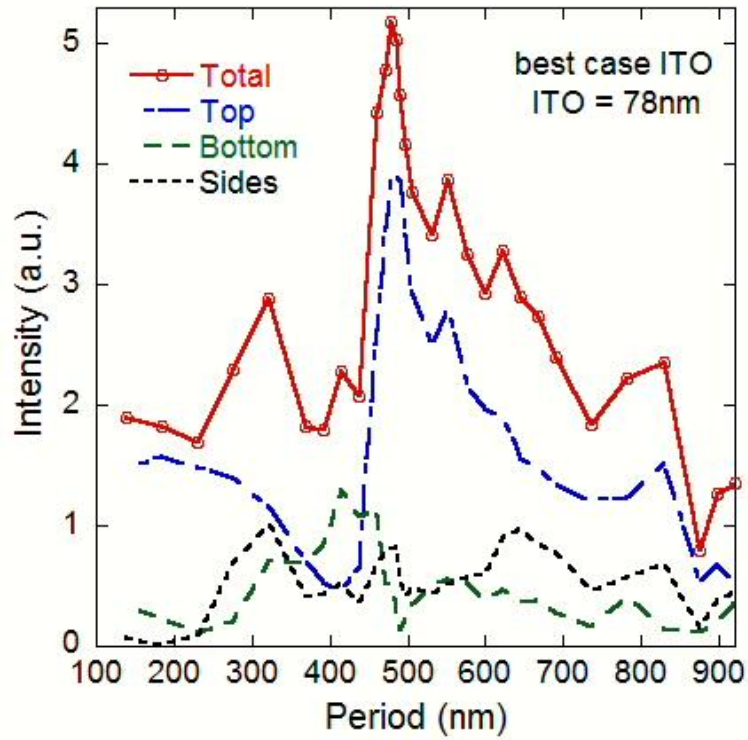


Figure 21 Total light intensity vs. grating period on a best case ITO of 78nm with emission intensities for top, bottom, and sides.

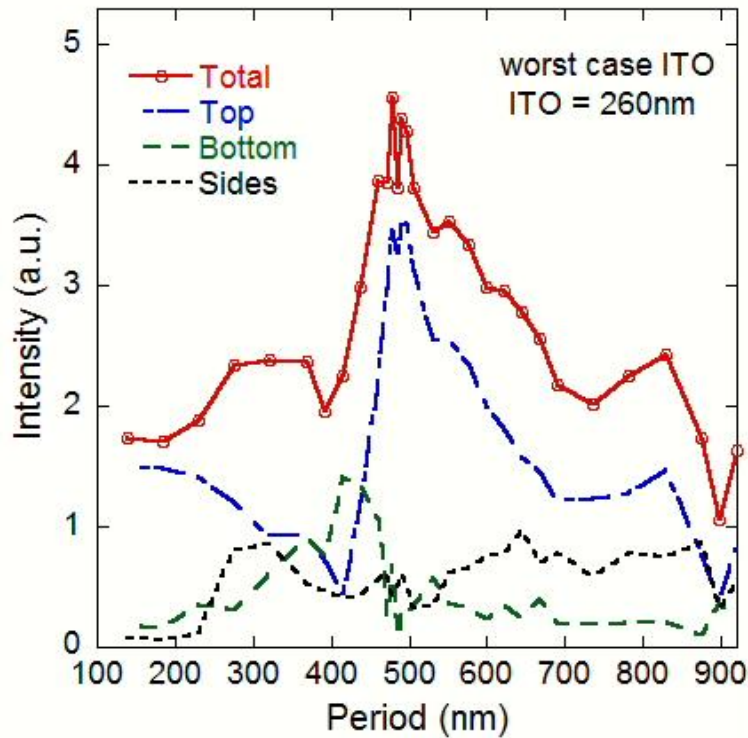


Figure 22 Total light intensity vs. grating period on a worst case ITO of 260nm with emission intensities for top, bottom, and sides.

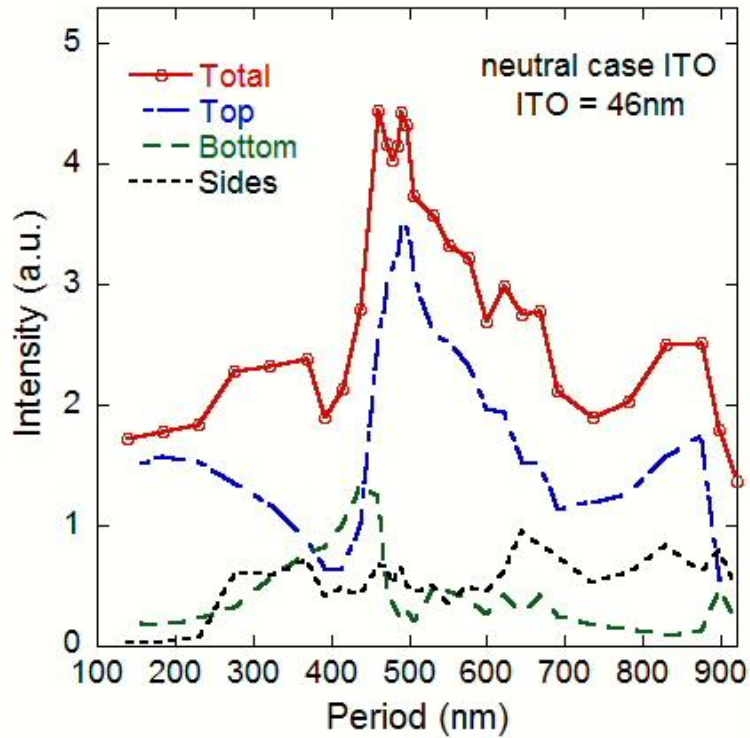


Figure 23 Total light intensity vs. grating period on a neutral case ITO of 46nm with emission intensities for top, bottom, and sides.

From the above graphs we see that best total light emission occurs when the grating is implemented on the best case ITO, Figure 21. And unlike the other two cases in Figure 22 and Figure 23 where the neutral and worst case ITO thicknesses spread total light emission maxima into two separate, less intense peaks, the best case total and top light emission peaks occur at the same grating period. When top light intensity decreases, bottom light output dramatically increases as seen in the transition from 500nm to 400nm. This sharp increase in bottom light emission causes the dual peak in total light emission for the neutral and worst case ITO thicknesses because the top light emission is still strong while bottom light emission rapidly increases.

The steady state electric fields of the best and worst grating periods for top light emission in Figure 24 and Figure 25, resemble the steady state electric fields produced in the standing wave analysis's best and worst top emission cases. The grating period that

gives the best top light output and a low bottom light output shows an extreme concentration of electromagnetic radiation around the triangles of the grating and very little radiation in the area below the MQW region. However, when the worst grating period is used (still on best case ITO), there is little electromagnetic activity around the grating. Instead, strong wave patterns are observed in the sapphire substrate and the largest bottom light output is observed (for best case ITO).

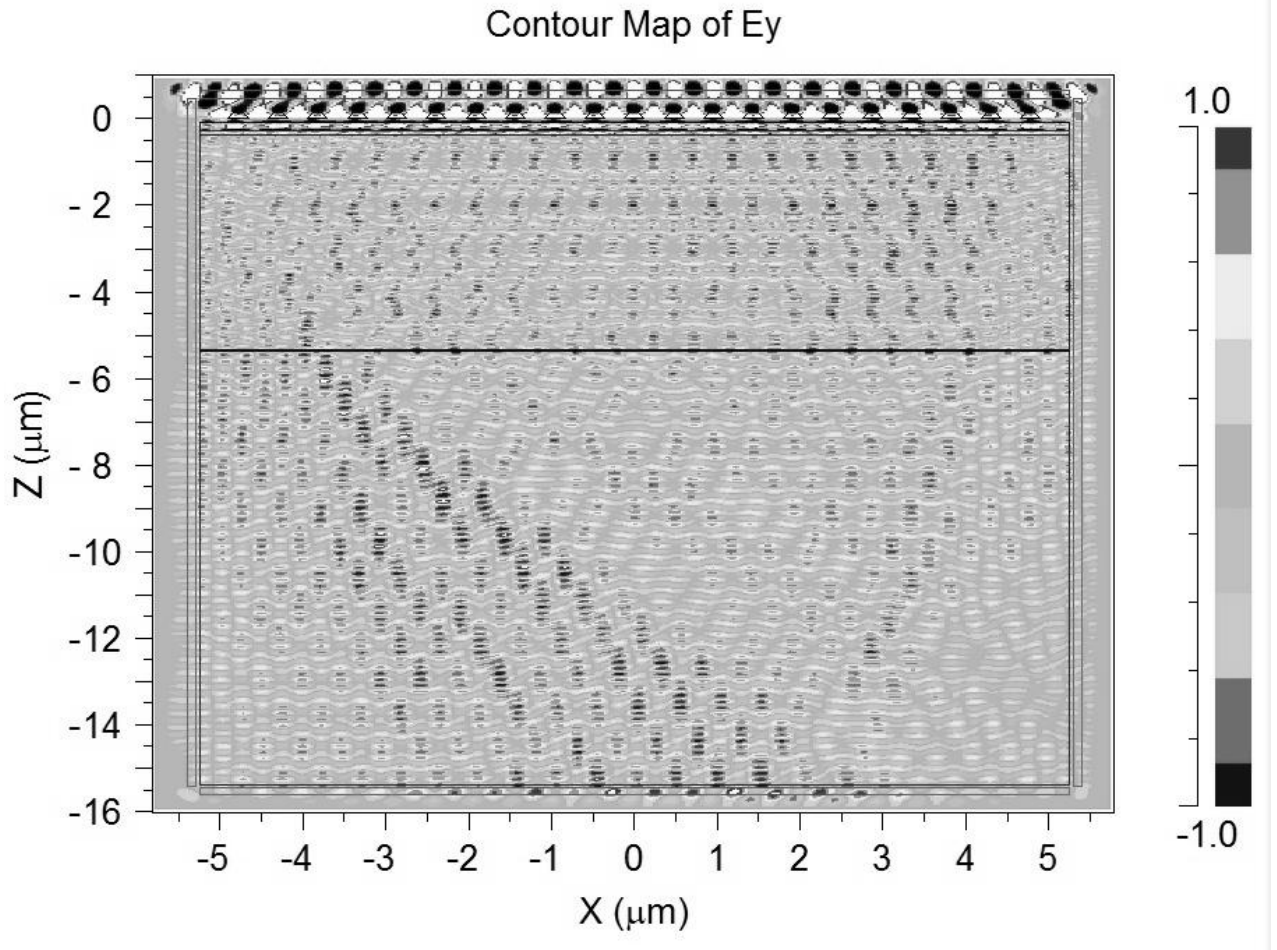


Figure 24 Steady state electric field in LED using best grating for top light extraction and best case ITO. Period = 478nm, ITO = 78nm.

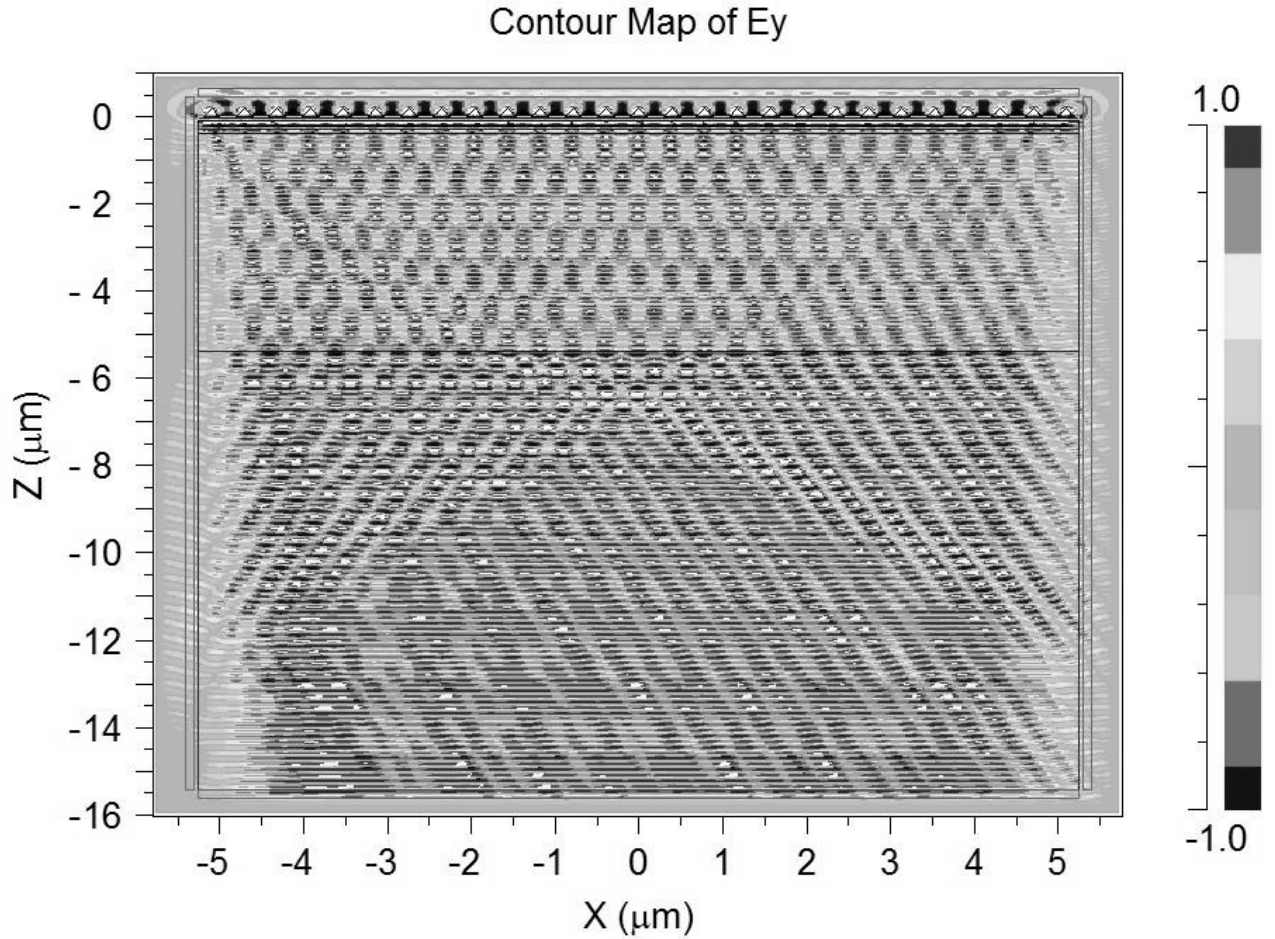


Figure 25 Steady state electric field in LED using worst grating for top light extraction and best case ITO. This period also produced the highest bottom light output. Period = 388nm, ITO = 78nm.

Gratings and Substrate Variation

I next combined key points from the substrate standing wave analysis with the grating simulations, again measuring all light extracted from the LED. An ITO thickness of 78nm is used because it maximizes standing wave interference patterns in the LED. Substrate thicknesses of 10,033nm, 10,050nm, and 10,064nm are chosen because they respectively minimize top light extraction, maximize top extraction, and maximize total light extraction.

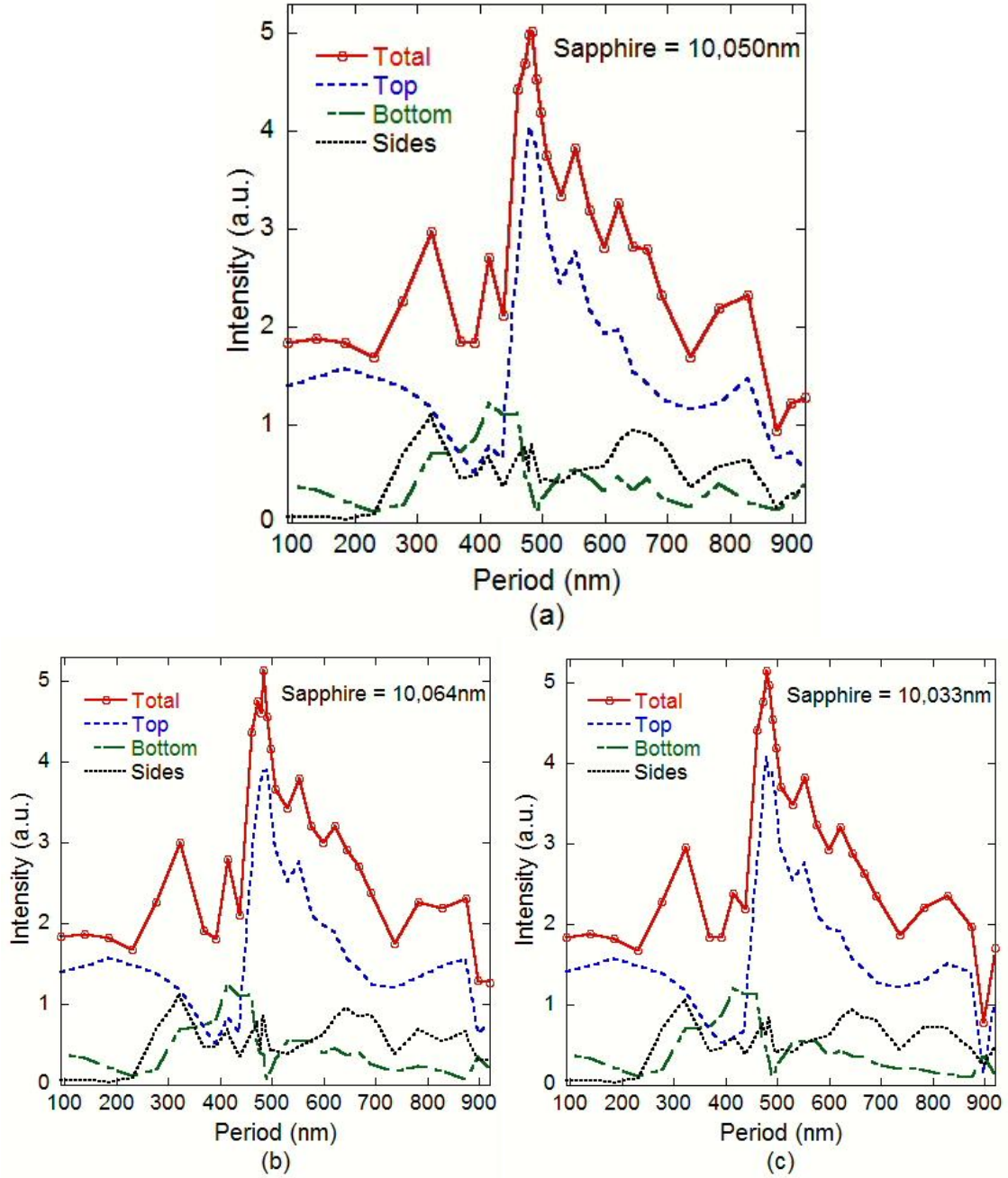


Figure 26 Grating total light extraction on three different sapphire substrate thicknesses with ITO = 78nm. a) best standing wave top light extraction, sapphire = 10,050nm, b) best standing wave total light extraction, sapphire = 10,064nm, and c) worst standing wave top extraction, sapphire = 10,033nm.

The results from these three simulations show remarkably similar light output patterns, even though the sapphire's standing wave analysis showed that they had very different outputs. This similarity is a result of the grating exerting a much stronger

influence on light output from the LED than the standing waves do. It shows that variation caused by differences in ITO thickness, section 5.3, is much more influential than sapphire substrate variation when a grating is added. This occurs even though larger standing wave minima and maxima were reached through sapphire variation and a best case ITO thickness than were reached with worst or thin case ITO. An important process to note is that adding the grating triangles to the LED changes the equivalent thickness of the ITO layer.

The gratings key light output intensities are listed in Table 9 and compared to the two references in Table 10. From Table 10, we see that the substrate thickness can change the grating's percent increase over reference 2 by 14-16%. By implementing gratings on the sapphire substrate thicknesses chosen from the standing wave analysis, we expected to obtain three distinct results (the 10,000nm results are from Section 5.3). The 10,050nm thickness should have provided the best top light output by the standing wave analysis, and the 10,064nm layer should have had the largest total light output. These two thicknesses did behave as expected, however, the grating results on the 10,033nm thickness actually produced slightly higher top and total outputs than either of them; even though the standing wave results indicated that this should have produced the lowest top light output. Also, the 10,033nm case's total light output peak occurs at the same grating period as its top light emission peak while the other thicknesses had slightly offset top and total peaks. These results show that the grating can change the standing wave patterns effect on light output beyond what we expect from a non-grating standing wave analysis.

Table 9 Light extraction minima and maxima for the LED with gratings on differing sapphire substrate thicknesses. ITO = 78nm

Light Emission (a.u.)	Sapphire Substrate Thickness (nm)			
	10,000	10,033	10,050	10,064
Best Top period = 490/478/478/490nm	3.8947	4.0756	4.0558	3.9065
Worst Top period = 898/898/392/392nm	0.45608	0.14749	0.51527	0.51538
Total @ best top grating period	5.04168	5.14659	4.9963	4.567849
Best Total period = 484/478/484/484nm	5.17865	5.14659	5.02426	5.13402

Table 10 Percent improvement of top light emission by grating at top light extraction maxima for different sapphire substrate thicknesses and top emission efficiency as % of total emission at top emission maxima. ITO = 78nm.

	Sapphire Substrate Thickness (nm)			
	10,000	10,033	10,050	10,064
% imp. over ref. 2, the conventional LED	238.7	254.4	252.7	239.7
% imp. over best SW case	209.0	223.4	221.8	209.9
top emission efficiency as % of total emission at top emission maxima	77.3	79.2	81.2	85.5

Combining nano-scale gratings with the key material thicknesses found in the standing wave analysis allows us to increase top light extraction to 4.076, a 254.4% improvement over reference 2's 1.150 a.u. output, and a 223.4% improvement over the best standing wave's output of 1.260 a.u. At peak light output, the grating not only increases top light emission, but also cause 79.2% of all light emitted from the top of the LED to exit from the top. This preferential output shows that the device can efficiently direct light and operate at a much higher light extraction efficiency when using a grating period of 478nm.

Grating output at different wavelengths

Because LEDs output light over a range of wavelengths surrounding the primary wavelength as seen in Figure 3, we must verify that the grating period that maximizes light extraction at the center wavelength is still effective at other wavelengths in the primary emission range. To better understand how the wavelength of light affects light output, the grating periods around peak light emission are re-simulated at free space wavelengths of 470nm and 450nm. These are wavelengths that are near the peak wavelength of 460nm and are still strongly emitted by the LED. These simulations use an ITO thickness 78nm and a sapphire substrate thickness of 10,050nm.

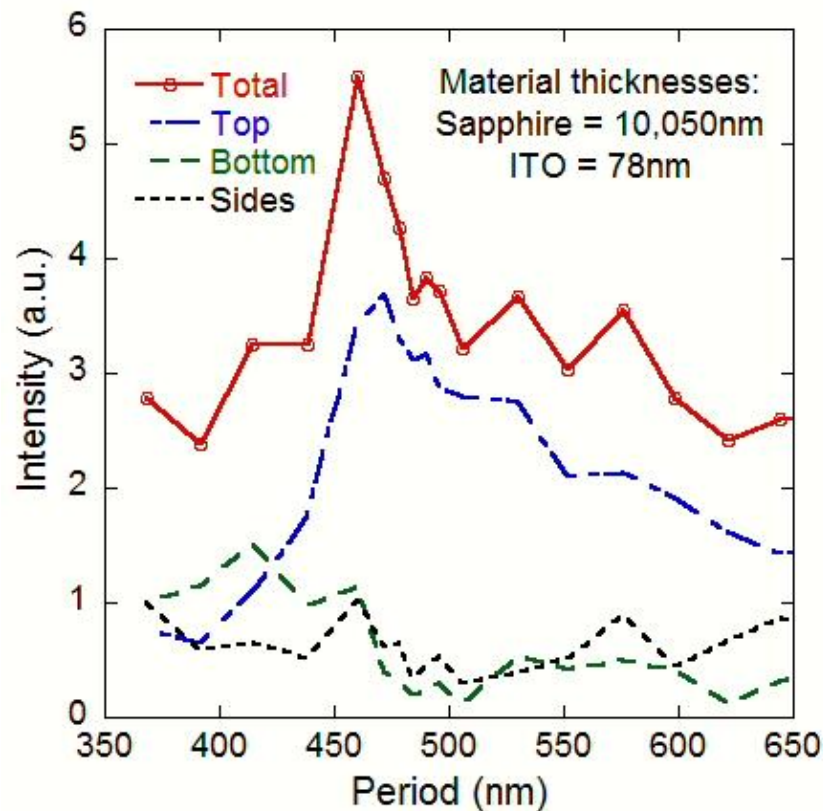


Figure 27 Grating total light output when free space wavelength is 450nm.

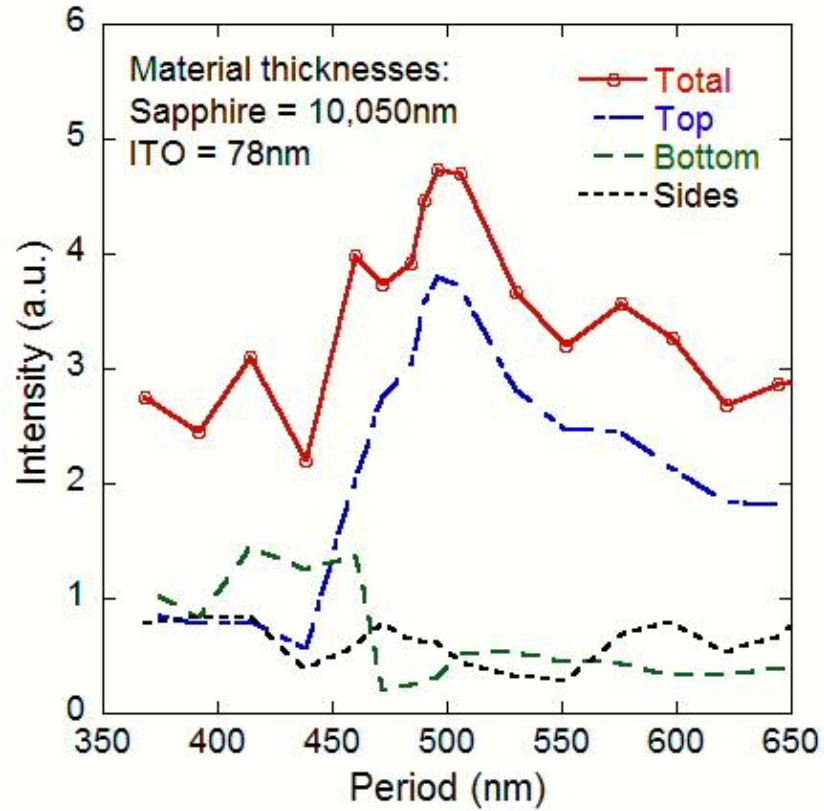


Figure 28 Grating total light output when free space wavelength is 470nm.

The gratings results from Figure 27 and Figure 28 show that the gratings are still highly effective at increasing the light output from the LED for both 450nm light and 470nm light. And total light extraction in Figure 27, with $\lambda_o = 450\text{nm}$, is substantially higher than any total light extraction that was achieved for either the 460nm or 470nm light since the shoulder of the top emission peak overlaps with a sharp rise in light extraction from both the bottom and sides of the LED.

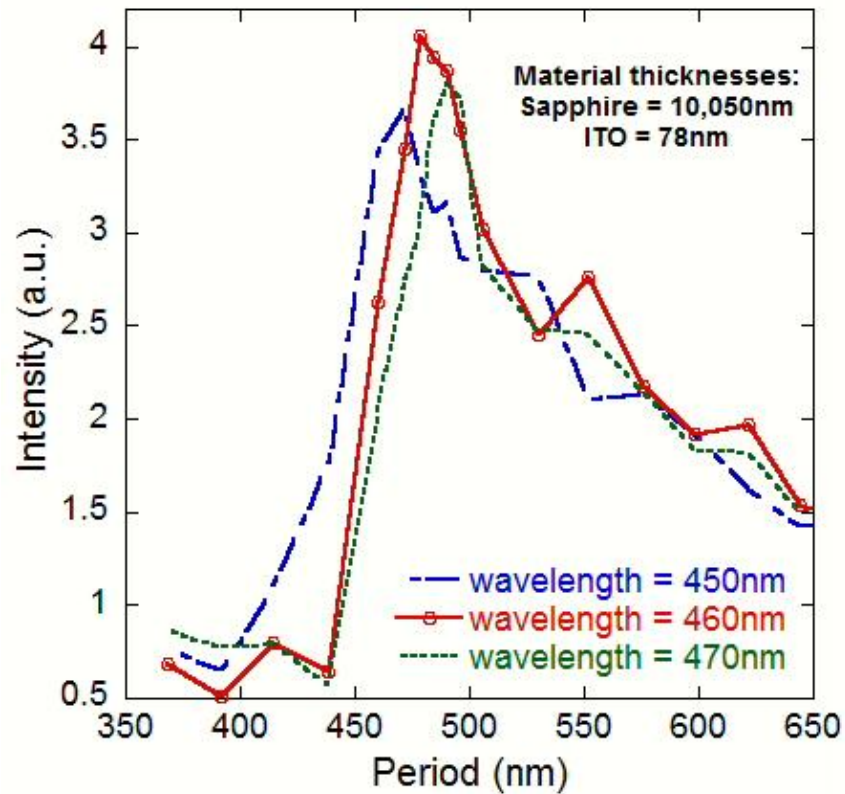


Figure 29 Comparing grating light outputs for three LED wavelengths.

When the light extraction for all three wavelengths is graphed in Figure 29, the light extraction peak clearly shifts with wavelength. But, since the light extraction peaks closely overlap with each other, the grating period that maximizes light extraction at $\lambda = 460\text{nm}$, 478nm , will still significantly improve light extraction within the GaN range of emitted wavelengths.

The peak grating light output is most likely lower at $\lambda = 450\text{nm}$ & 470nm because the ITO and sapphire thicknesses used in these models were optimized for a wavelength of 460nm during standing wave analysis. Changing the wavelength of light in the LED model will change how the standing wave interferes at the LED surface. To reach the output intensity achieved with 460nm light, standing wave analysis must be performed on the LED to optimize the material thicknesses at that wavelength.

Explaining the grating results

In general, as the grating period decreases towards the free space wavelength of the light used in the simulation, the top light output increases. But top light output plummets as the grating period passes the free space wavelength before gradually increasing again. This may be the result of two different phenomena: the grating providing additional angles and surface area for light to escape from, and the grating effectively acting as a graded index of refraction between ITO and air.

The large light extraction intensity points to the grating providing additional angles and surface area for light to escape the LED surface. The light output then increases as triangle density increases and grating period decreases. However, as the decreasing space between triangles approaches $\frac{\lambda}{2}$, the light that perpendicularly approaches the ITO to air interface and previously escaped the LED now strikes some portion of an ITO triangle. This light then strikes the side of the triangle below the critical angle and reflect back into the LED. The significant increase in bottom and side light emission after the grating period decreases past the wavelength of light seems to support this hypothesis.

On the other hand, the gradual increase in light extraction below a grating period of 400, shown in Figure 26, can be interpreted as the effect of another phenomena. As the grating period becomes significantly shorter than the wavelength of light the triangles in the grating can be viewed as creating an effective gradient between the index of refraction of ITO and air. At the base of the triangles, the effective index of refraction equals that of ITO while at the tip of the triangle, the effective index of refraction is finishing its transition to the air's index of refraction. As the grating period shrinks, the

triangle density increases, causing a better transition between the indices of ITO and air. But as the grating period continues to shrink, the triangle height becomes too small to effectively penetrate into the air and provide the transition between indices of refraction. This effect causes the grating to extract less light as period approaches 92nm.

CHAPTER 6: CONCLUSION

This thesis used three methods to improve GaN LED light extraction: first, by adding ITO the surface to increase the critical angle of light exiting the LED. Second, by optimizing the ITO and sapphire thicknesses based on standing wave analysis. And third, by adding ITO transmission gratings to the LED over a range of grating periods.

The first portion of the study indicated that adding the ITO layer did improve light extraction efficiency. However, the effect of increasing critical angle could not be sufficiently separated from the standing wave effects of adding ITO to clearly determine how much increasing critical angle affected light extraction. The second portion of the study showed that standing waves exist in the LED and are modified by ITO and sapphire thicknesses. Changing these thickness caused the light output to vary from 0.809 to 1.260 a.u. and showed that the light output could decrease by 15.4% from the unmodified reference LEDs 1.150 a.u. output. However, the best standing wave case showed that light extraction can improve by 9.6% over the unmodified LED and by 55.8% over the worst case standing wave output. The third portion of this study showed that adding gratings to the LED can significantly increase or decrease light output intensity depending on the period used. The best grating case increased light output by 222% over the best standing wave output.

We find that the final combination of increased critical angle, best case standing wave, and best grating period can improve light output by 253% over the conventional LED. This significant increase in light extraction efficiency justifies the increase in complexity required to fabricate the LEDs and shows that the GaN LED can continue increasing its efficiency to meet the lighting demands of our future.

CHAPTER 7: FUTURE WORK

This thesis only investigated the 50% fill factor in order to focus on standing wave and the effect of grating period. However, future work should study the effect of fill factor on grating extraction efficiency at different periods. In the standing wave analysis shown in Figure 10, the sinusoid shows roughness and appears to jump between values. Future work could improve these results by simulating the model at a higher mesh resolution since the higher resolution will better capture the effect of multiple reflections at each material interface. This should smooth out the jumps seen in the graph for the 1nm changes in ITO thickness.

The effect of adding a reflecting metal layer to the bottom of the LED should be investigated with standing wave analysis. The reflection layer should then be combined with grating analysis to see how the reflection layer effects grating light emission. Other grating shapes must also be studied besides the triangle to determine how grating shape changes maximum light output and to determine what the ideal grating period is for the different grating shapes. Studying these gratings in three dimensions, while more computationally extensive and time consuming can increase the simulations accuracy and better represent the effect an LED.

LEDs emit light over a range of wavelengths, in order to better test this phenomena, the standing wave analyses and grating simulations should be done at several wavelengths emitted by the LED to verify their behavior over the emission range of the LED. One method of doing this is to inject light at three wavelengths that characterize the LEDs emission like 450nm, 460nm, and 470nm. Or, a better way to characterize the optical light emission efficiency of an LED with a 460nm center wavelength is to

measure the grating's light extraction efficiency over many different wavelengths between 430nm and 490nm. This will allow the gratings light extraction efficiency to be determined over the entire effective light emission range of the LED.

PUBLICATIONS

- [1] *Gabriel Halpin*, Xiaomin Jin, Xing-Xing Fu, Xiang-Ning Kang, and Gou-Yi Zhang, "Study of top ITO nano-gratings on GaN LEDs", 13th IEEE International Conference on Nanotechnology, Beijing, China, August 2013.
- [2] *Gabriel Halpin*, Xiaomin Jin, Greg Chavoor, Xing -Xing Fu, Xiang-Ning Kang, and Gou-Yi Zhang, "Simulation of nanoscale ITO top grating of GaN LED," SPIE Photonics West 2013, Proc. Vol. 8619: Phys. & Sim. of Optoelectronic Dev. XXI. February 2013.
- [3] J. P. Sharpe, T. Post, S. Khatri, & *G. Halpin*. "Fabrication and characterization of optical waveguides and grating couplers," 2013 *Eur. J. Phys.* 34 1317.
- [4] Travis Robinson, Xiaomin Jin, *Gabriel Halpin*, Xiang-Ning Kang, and Gou-Yi Zhang, "Top ITO nano transmission grating GaN LED simulations for light extraction improvement," Accepted to SPIE Photonics West 2014. Paper #8980-66.
- [5] *Gabriel Halpin*, Travis Robinson, Xiaomin Jin, Xiang-Ning Kang, and Gou-Yi Zhang, "Study of GaN LED ITO Nano-grating with Standing Wave Analysis," In preparation for OSA's Chinese Optics Letters.

REFERENCES

- [1] Navigant Consulting, Inc., "Energy savings potential of solid-state lighting in general illumination applications," *U.S. Energy Information Administration (EIA), Office of Energy Efficiency*. Web. 25 Oct. 2013.
<http://apps1.eere.energy.gov/buildings/publications/pdfs/ssl/ssl_energy-savings-report_jan-2012.pdf>
- [2] "Cree sets new R&D performance record with 276 lumen-per-watt power LED," *Cree News & Events (Feb. 2013)*. Web. 25 Oct. 2013.
- [3] D. A. Neamen, *Semiconductor Physics and Devices*. 4th ed. New York: McGraw Hill, 2012. ch. 14.
- [4] R. F. Brown. *Solid State Physics: An Introduction for Scientists and Engineers*. San Luis Obispo, CA: El Corral Bookstore. 2009 ch. 7.
- [5] Cree, "LED color mixing: basics and background," web. accessed 12-2013, <http://www.google.com/url?sa=t&rct=j&q=&esrc=s&source=web&cd=1&ved=0CC4QFjAA&url=http%3A%2F%2Fwww.cree.com%2F~%2Fmedia%2FFiles%2FCree%2FLED%2520Components%2520and%2520Modules%2FXLamp%2FXLamp%2520Application%2520Notes%2FLED_color_mixing.pdf&ei=IVCqUrW5M4OgqgHk8YCYBA&usg=AFQjCNHGDCs9kg1dsRkYYF8wjcLDJWTvJw&sig2=e2XvqEQPXy5gx16brgYxAg&bvm=bv.57967247,d.aWM&cad=rja>
- [6] Ziquan Guo *et al.*, "Optimization Studies of Two-Phosphor-Coated White Light-Emitting Diodes," *Photonics Journal, IEEE* , vol.5, no.2, pp.8200112,8200112, April 2013.

- [7] N. Hirosaki, "Phosphor, production method thereof and light emitting instrument," U.S. Patent 11/659,789, Feb. 9, 2007.
- [8] S. S. Treiu, and X. Jin, "Study of top and bottom photonic gratings on GaN LED with error grating models," IEEE J. of Quantum Electronics, vol. 46, no. 10, pp. 1456-1463, Oct. 2010.
- [9] K. Bao *et al.*, "Improvement of light extraction from patterned polymer encapsulated GaN-based flip-chip light-emitting diodes by imprinting," IEEE Photonics Technol. Lett., vol. 19, No. 22, Nov. 2007.
- [10] H. W. Huang *et al.*, "Investigation of GaN-based light emitting diodes with nano-hole patterned sapphire substrate (NHPSS) by nano-imprint lithography," Materials Science and Engineering B, vol. 164, pp. 76-79, 2009.
- [11] W. Lin *et al.*, "Enhanced output power of near-ultraviolet InGaN/ AlGaN LEDs with patterned distributed Bragg reflectors," IEEE Transactions on Electron Devices, vol. 58, Jan. 2011.
- [12] Z. Wang *et al.*, "Double-grating displacement structure for improving the light extraction efficiency of LEDs," The Scientific World J., vol. 2012, article ID 515468, 2012.
- [13] Y. S. Yu *et al.*, "Effect of the silver mirror location on the luminance intensity of double-roughened GaN light-emitting diodes," Electrochemical and Solid State Lett., vol. 10, pp. J126-J128, 2007.
- [14] G. Chavoor *et al.*, "Light extraction improvement of GaN LEDs using nano-scale top transmission gratings," Proc. SPIE 8123, 11th International Conf. on Solid State Lighting, 81231A, Sept. 2011.

- [15] C. Lin *et al.*, "Light extraction enhancement of a GaN based light-emitting diode through grating-patterned photoelectrochemical surface etching with phase mask interferometry," *IEEE Photonics Technol. Lett.*, vol. 22, No. 9, May 2010.
- [16] T. Kim *et al.*, "Enhancement in external quantum efficiency of blue light-emitting diode by photonic crystal surface grating," *IEEE Electronics Lett.*, vol. 41, No. 20, Sept. 2005.
- [17] C.W. Kuo *et al.*, "Optical Simulation and Fabrication of Nitride-Based LEDs With the Inverted Pyramid Sidewalls," *Selected Topics in Quantum Electronics, IEEE Journal of*, vol.15, no.4, pp.1264,1268, July-Aug. 2009.
- [18] S.R. Kim *et al.*, "Potential environmental impacts from the metals in incandescent, compact fluorescent lamp (CFL), and light-emitting diode (LED) bulbs," *Environ. Sci. Technol.*, Jan. 2013.
- [19] M. Freebody, "LEDs: The greener choice, or a toxic threat?," *Photonics Spectra*. web. Accessed 12-2013. <<http://www.photonics.com/Article.aspx?AID=46650>>
- [20] F.L. Pedrotti & L.S. Pedrotti, *Introduction to Optics*. 2nd ed. Upper Saddle River, NJ: Prentice Hall, 1993, ch. 17.
- [21] P. Mouroulis, *Geometrical Optics and Optical Design*. New York: Oxford, 1997. ch. 6.
- [22] G. Chavoor, "Light extraction enhancement of GaN based LEDs using top grating, patterned sapphire substrates, and reflective surfaces," M.S. thesis, Dept. Electrical Engr., Cal Poly St. Univ., San Luis Obispo, CA, 2012.
- [23] RSoft, "The FDTD Algorithm," Fullwave 6.0 user guide.

[24] Wikipedia, "Finite-difference time-domain method", web. Accessed 12-2013,

<http://en.wikipedia.org/wiki/Finite-difference_time-domain_method>

[25] Remcom, "FDTD Method", web. Accessed 12-2013.

<<http://www.remcom.com/xf7-fdtd-method/>>

APPENDICES

Appendix A: Finite difference time domain method (FDTD)

The FDTD method breaks down the simulation space into discrete time and space cells and numerically solves Maxwell's equations to determine the electric and magnetic field components in each cell [23]. These time quantized spaces are called Yee cells, Figure 30, and models are meshed into grids of these cells before a simulation begins. The Yee cell side length represents the distance an electromagnetic field travels during one time step of the simulation. Because the electric and magnetic fields are offset, the simulation calculates first one and then the other in a leapfrog scheme as the EM wave travels through the model [24].

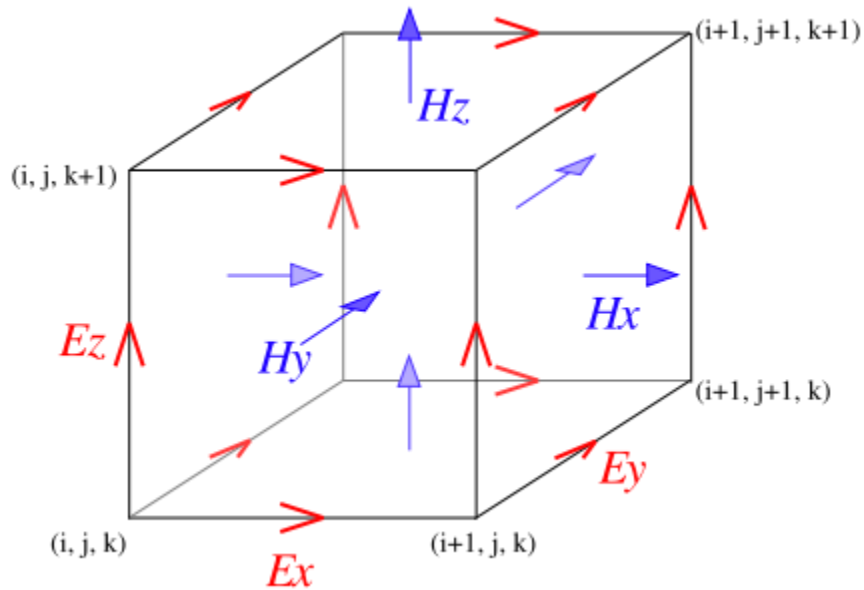


Figure 30 The Yee cell.

[23]

Because the cell side length limits the upper frequency of EM radiation that can be calculated, the side wall length must be at least one-tenth the length of the wavelength being studied [25]. The Yee cell size also limits the size of the smallest feature that can be accurately simulated in the CAD model. For sub-wavelength feature sizes, the mesh used must be smaller than the smallest feature size used.

Appendix B: RSoft - Building and Simulating the Model.

The first step to building an LED with a triangle grating in RSoft CAD is building an individual triangle for the grating. Once built, this triangle will be used by the array generation tool to set up the grating. After building the triangle array (the grating), we will add the other components of the LED layer by layer beneath the array.

To begin, open a new file and in the first window set the free space wavelength to $0.46\text{ }\mu\text{m}$ (μm is the default unit in RSoft). Once in the new CAD space, create a material segment and right click on it. This will bring up the properties window shown in Figure 31. If the properties in the window are changed to match Figure 31's values, the material segment will change its shape to become the 460nm grating triangle in the figure.

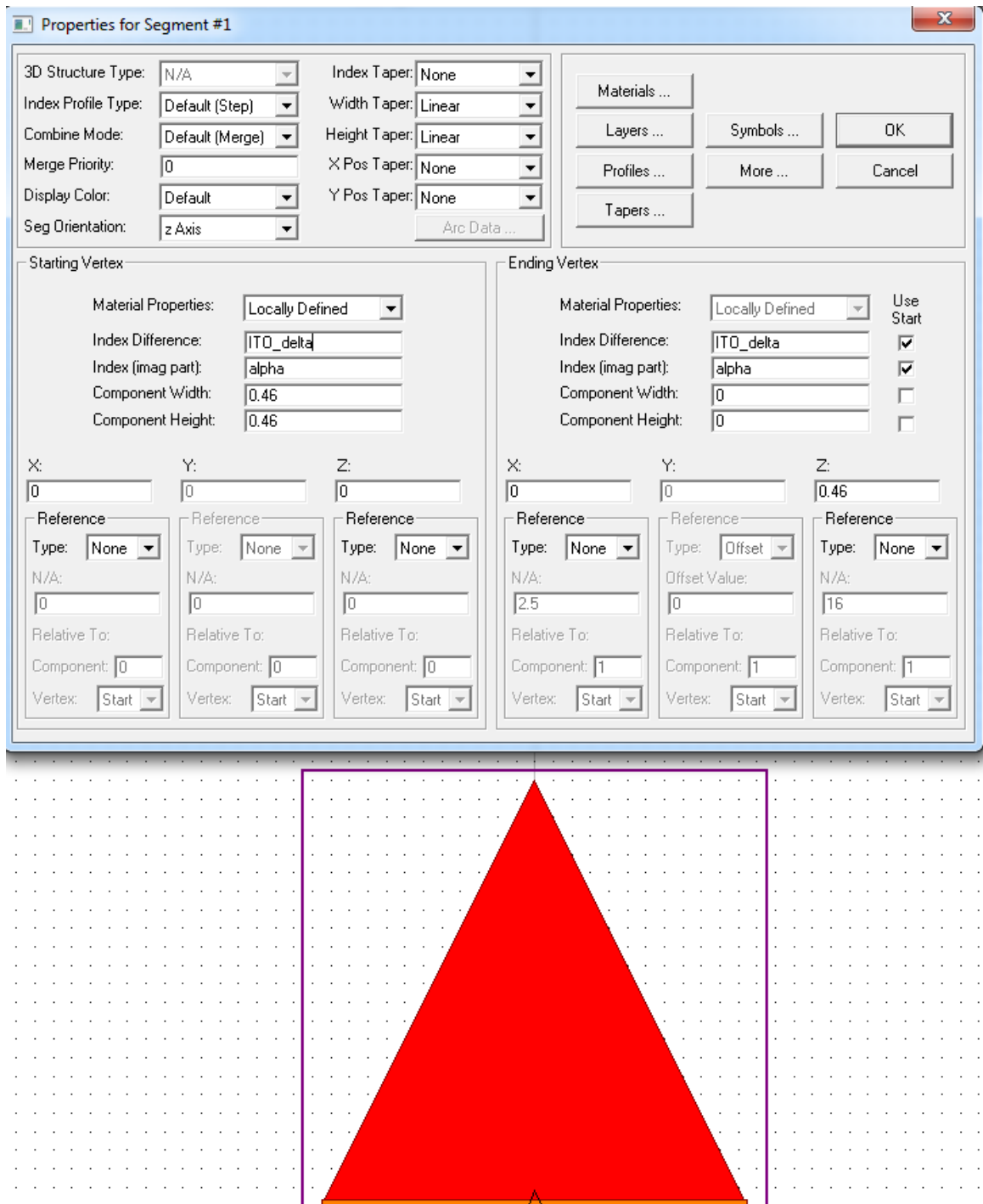


Figure 31 Making a grating triangle in CAD

Under 'Index Difference', note that a numeric answer is not given. Instead, I typed in a symbol name that I defined after clicking on the Symbol button in the top right corner. In the definition, $ITO_delta = 1.77 - \text{background index}$. I define the index

difference this way to make it easy to check that I have defined the material correctly when building the LED model. Also, by defining the index difference in terms of the index of refraction of ITO, 1.77, and the variable 'background index' simulating the LED emitting into a non-air environment like epoxy becomes as easy as changing the background index variable. When this is done, save the triangle as a CAD object with a .ind file name, the default.

Next, on the top bar open 'Utility' and select 'Array Layout...'. This will take you to the screen in Figure 32. For the lattice dimensions, we make sure the array is created in the XY plane using the triangle created in the previous step as the unit cell. Because the LED model dimensions are fixed throughout the study, we must calculate how many triangles can fit on the top of the LED. To get a rough estimate, divide the LED width by the grating period as seen in Eq. B.1.

$$\frac{LED\ width}{grating\ period} = \frac{LED\ width}{cone\ size * 2} = \frac{10,500nm}{460nm * 2} = 11.41 \approx 11 \quad [B. 1]$$

To maintain symmetry, I always rounded to the nearest odd number of triangles that could fit on the device. Keep in mind that there is some leeway when you decide to round the number of triangles up or down the grating triangles can get very close to the LED edge. The blank space left for the 50% fill factor can run over the LED edge since it is the material-less region of the grating. Finally, enter the output prefix that the new array will be saved as and click 'Ok'.

Note: the triangle file (or a copy with the same file name) must remain in the same folder as the array for the array to function.

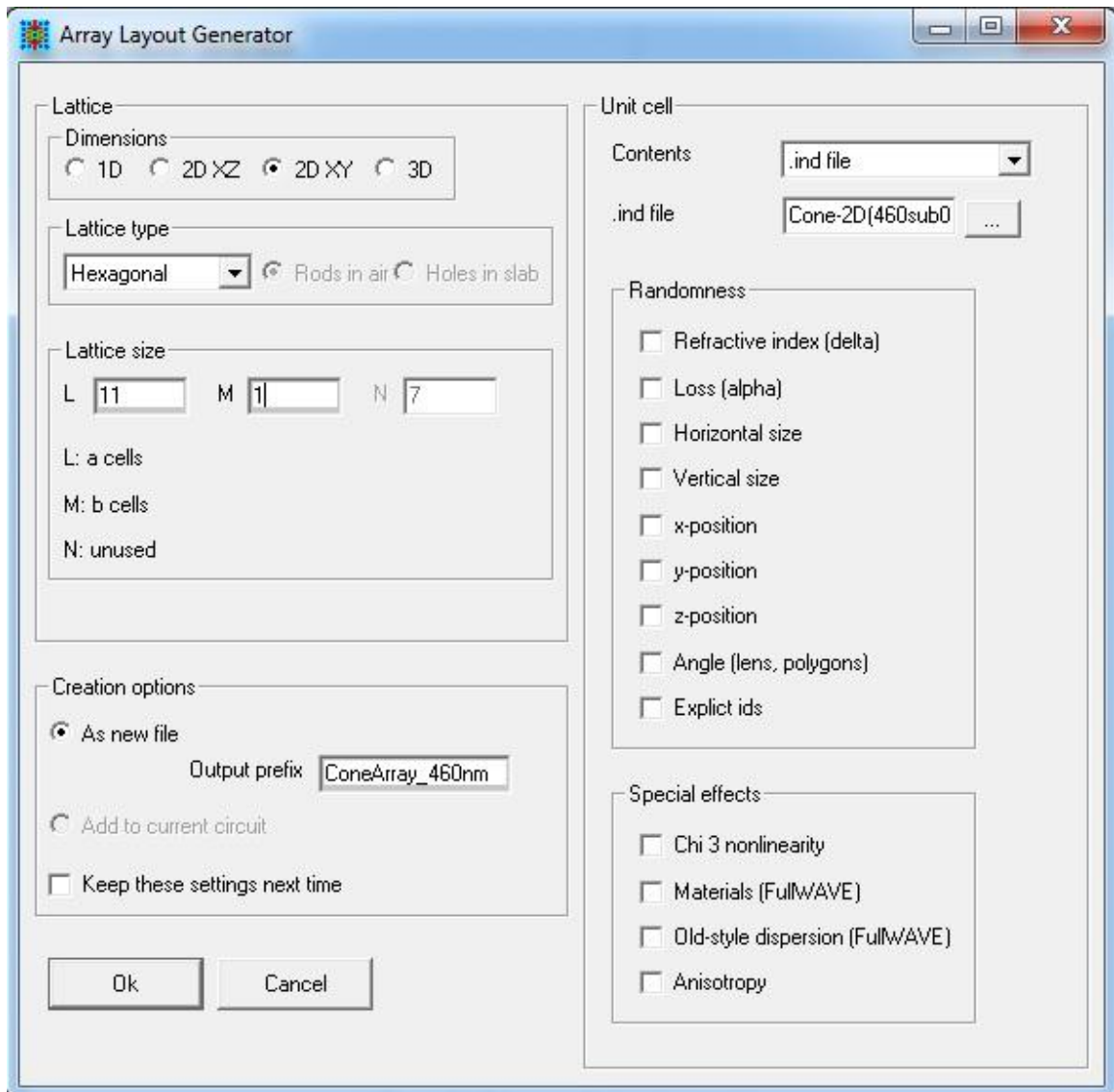


Figure 32 The array layout generator.

When generated, the array will look like Figure 33. While this grating doesn't look like the grating that should be created, observe the aspect ratio shown in the top right corner and change it to 1:1.

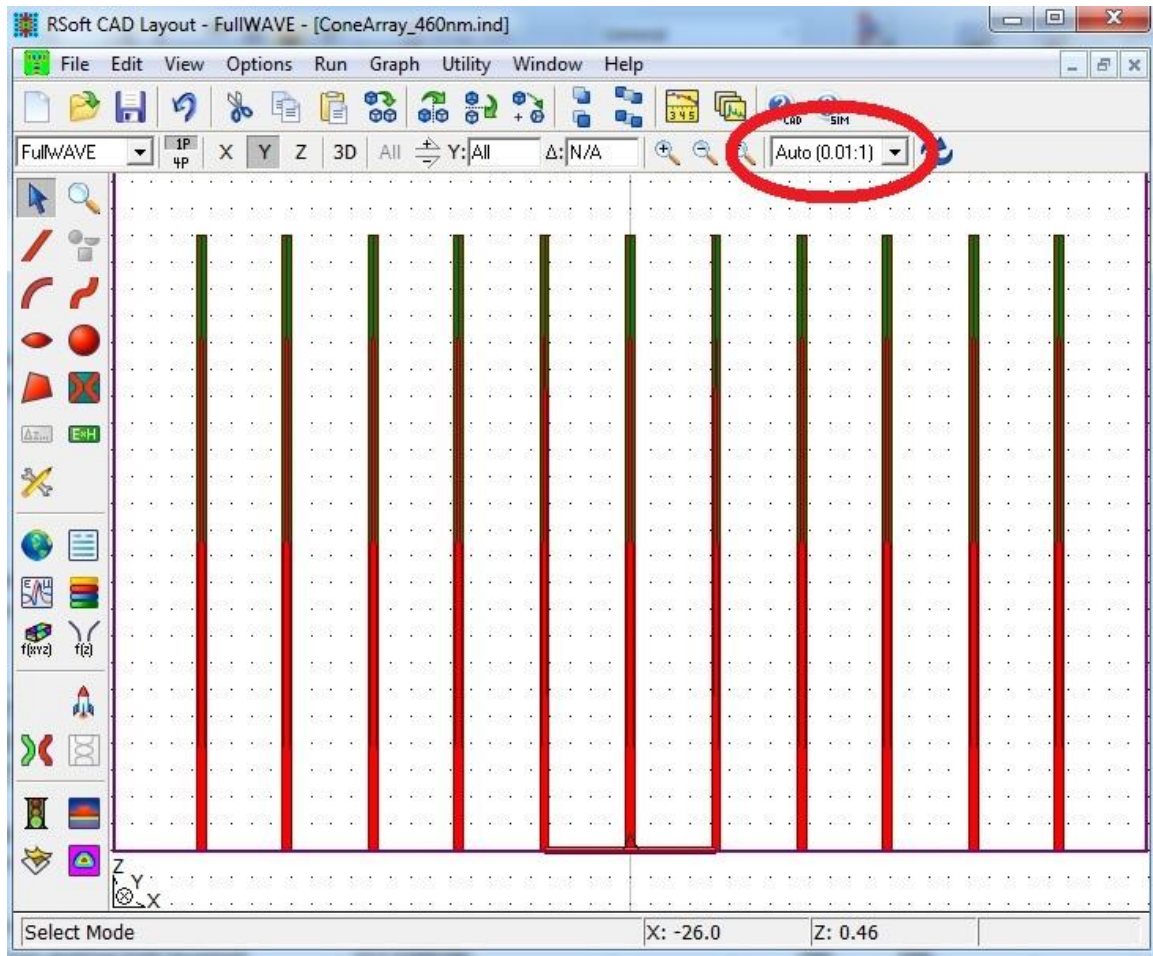


Figure 33 The newly generated triangle array.

With the corrected aspect ratio shown in Figure 34, we see that the grating period must be fixed before we build the rest of the LED underneath the array.

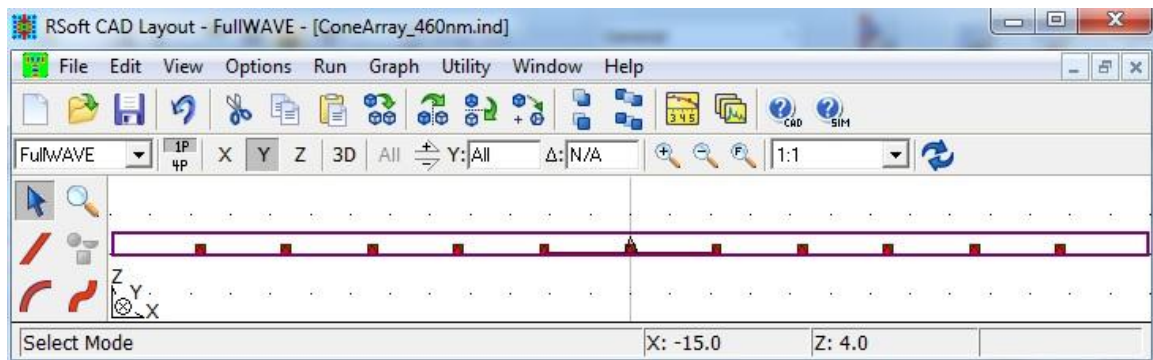


Figure 34 The newly generated triangle array at a 1:1 aspect ratio.

The next step is done easiest in a text editor like notepad so shut the CAD window and reopen it with Notepad or a similar program like Notepad ++. When opened, you will see the large, confusing set of text that defines the CAD model - see Grating Code. However, learning to change key items in this text based format will save a lot of time when you build future models since you can copy and paste many parameters from previous model files into each new one you build. This is important because for every grating data point you must make a new grating model. For this first model, observe the commented items in the list.

Grating Code 1

```
A = Period
Ax = A*sin(PhiPattern+PhiA)
Ay = A*cos(PhiPattern+PhiA)
Az = 0
B = A
Bx = B*sin(PhiPattern+PhiB)
By = B*cos(PhiPattern+PhiB)
Bz = 0
C = A
CellVolume = abs(Ax*(By*Cz-Bz*Cy)+Ay*(Bz*Cx-Bx*Cz)+Az*(Bx*Cy-By*Cx))
Cx = 0
Cy = 0
Cz = 1
DomainX = PeriodX
DomainY = 2*PeriodY
Dx = PeriodX/16
Dy = Dx*PeriodY/PeriodX
Dz = 0.5
NX = 11                                *number of triangles in X direction of array
NY = 1                                *number of triangle layers in Y direction
OffsetX = 0*Period
OffsetY = 0*Period
OffsetZ = 0*Period
Period = 4.3                           *change this to '2*.46' to achieve correct
                                       *grating period

PeriodX = Ax
PeriodY = By
PhiA = 90
PhiB = 30
PhiCell = 0
PhiPattern = 0
Xmax = (NX+1)/2*PeriodX
Xmin = -Xmax
Ymax = (NY+1)/2*PeriodY
Ymin = -Ymax
```

```

alpha = 0
background_index = 1          *this should be '1' for an air background
boundary_max = Xmax
boundary_max_y = Ymax
boundary_min = Xmin
boundary_min_y = Ymin
cad_aspectratio_y = 1
cad_yselect_size = PeriodY
char_nmax = 2
char_nmin = 0.5
color_outline = 0
delta = 1-background_index   *don't use this delta in material
                               definitions
                               *use custom definitions for each material

dimension = 3
free_space_wavelength = .46  *needs to be .46 for the blue wavelength
of GaN                       *LEDs
grid_size = Dx
grid_size_y = Dy
height = width
k0 = (2*pi)/free_space_wavelength
kbar = k0*Neff
lambda = free_space_wavelength
launch_height = launch_width
launch_position = 0
launch_position_y = 0
launch_type = LAUNCH_GAUSSIAN *change to LAUNCH_RECTANGLE
launch_width = 2*Period      *change to width
pbp_layout = PBG_LAYOUT_HEX_XY
profile_type = PROF_STEPINDEX
sim_tool = ST_FULLWAVE        *make sure this is ST_FULLWAVE
slice_display_mode = DISPLAY_CONTOURMAPXY
slice_grid_size = Dx
slice_grid_size_y = Dy
slice_output_format = OUTPUT_NONE
slice_step_size = Dz
step_size = Dz
width = 5                    *change to 10.5(μm) for all models in this thesis

*the following circuit references are created by the array generator
*and should not be changed after array is made
circuit_reference 1          end circuit_reference
    profile_type = PROF_INACTIVE
    color = 2
    reference_angle = PhiCell
    begin.x = -5*Ax+0*Bx+OffsetX
    begin.y = -5*Ay+0*By+OffsetY
    begin.z = 0
    indfile = Cone-2D(460sub000nm-
460nm)T2.ind
end circuit_reference

circuit_reference 2
    profile_type = PROF_INACTIVE
    color = 2
    reference_angle = PhiCell
    begin.x = -4*Ax+0*Bx+OffsetX
    begin.y = -4*Ay+0*By+OffsetY
    begin.z = 0
    indfile = Cone-2D(460sub000nm-
460nm)T2.ind

circuit_reference 3
    profile_type = PROF_INACTIVE
    color = 2
    reference_angle = PhiCell
    begin.x = -3*Ax+0*Bx+OffsetX
    begin.y = -3*Ay+0*By+OffsetY
    begin.z = 0
    indfile = Cone-2D(460sub000nm-
460nm)T2.ind
end circuit_reference

circuit_reference 4
    profile_type = PROF_INACTIVE
    color = 2
    reference_angle = PhiCell
    begin.x = -2*Ax+0*Bx+OffsetX
    begin.y = -2*Ay+0*By+OffsetY
    begin.z = 0

```

```

        indfile = Cone-2D(460sub000nm-
460nm)T2.ind
end circuit_reference

circuit_reference 5
    profile_type = PROF_INACTIVE
    color = 2
    reference_angle = PhiCell
    begin.x = -1*Ax+0*Bx+OffsetX
    begin.y = -1*Ay+0*By+OffsetY
    begin.z = 0
    indfile = Cone-2D(460sub000nm-
460nm)T2.ind
end circuit_reference

circuit_reference 6
    profile_type = PROF_INACTIVE
    color = 2
    reference_angle = PhiCell
    begin.x = 0*Ax+0*Bx+OffsetX
    begin.y = 0*Ay+0*By+OffsetY
    begin.z = 0
    indfile = Cone-2D(460sub000nm-
460nm)T2.ind
end circuit_reference

circuit_reference 7
    profile_type = PROF_INACTIVE
    color = 2
    reference_angle = PhiCell
    begin.x = 1*Ax+0*Bx+OffsetX
    begin.y = 1*Ay+0*By+OffsetY
    begin.z = 0
    indfile = Cone-2D(460sub000nm-
460nm)T2.ind
end circuit_reference

circuit_reference 8
    profile_type = PROF_INACTIVE
    color = 2

        reference_angle = PhiCell
        begin.x = 2*Ax+0*Bx+OffsetX
        begin.y = 2*Ay+0*By+OffsetY
        begin.z = 0
        indfile = Cone-2D(460sub000nm-
460nm)T2.ind
end circuit_reference

circuit_reference 9
    profile_type = PROF_INACTIVE
    color = 2
    reference_angle = PhiCell
    begin.x = 3*Ax+0*Bx+OffsetX
    begin.y = 3*Ay+0*By+OffsetY
    begin.z = 0
    indfile = Cone-2D(460sub000nm-
460nm)T2.ind
end circuit_reference

circuit_reference 10
    profile_type = PROF_INACTIVE
    color = 2
    reference_angle = PhiCell
    begin.x = 4*Ax+0*Bx+OffsetX
    begin.y = 4*Ay+0*By+OffsetY
    begin.z = 0
    indfile = Cone-2D(460sub000nm-
460nm)T2.ind
end circuit_reference

circuit_reference 11
    profile_type = PROF_INACTIVE
    color = 2
    reference_angle = PhiCell
    begin.x = 5*Ax+0*Bx+OffsetX
    begin.y = 5*Ay+0*By+OffsetY
    begin.z = 0
    indfile = Cone-2D(460sub000nm-
460nm)T2.ind
end circuit_reference

launch_field 1
    launch_pathway = 0
    launch_type = LAUNCH_GAUSSIAN
    launch_tilt = 0
    launch_mode = 0
    launch_mode_radial = 1
    launch_width = 2*Period
    launch_height = launch_width
    launch_position = 0
    launch_position_y = 0
end launch_field

```

*change to LAUNCH_RECTANGLE

*change to width

After modified the text file, the next step is adding the LED material layers beneath the array. Following the steps to make the triangle for the grating, add a segment to the CAD model and change its parameters to match the properties show in Figure 35.

may have overlapping layers or air gaps between layers when ITO thickness is varied.

Repeat these building steps all the way through the model to complete the model and add the material index difference and height variables for each layer as needed.

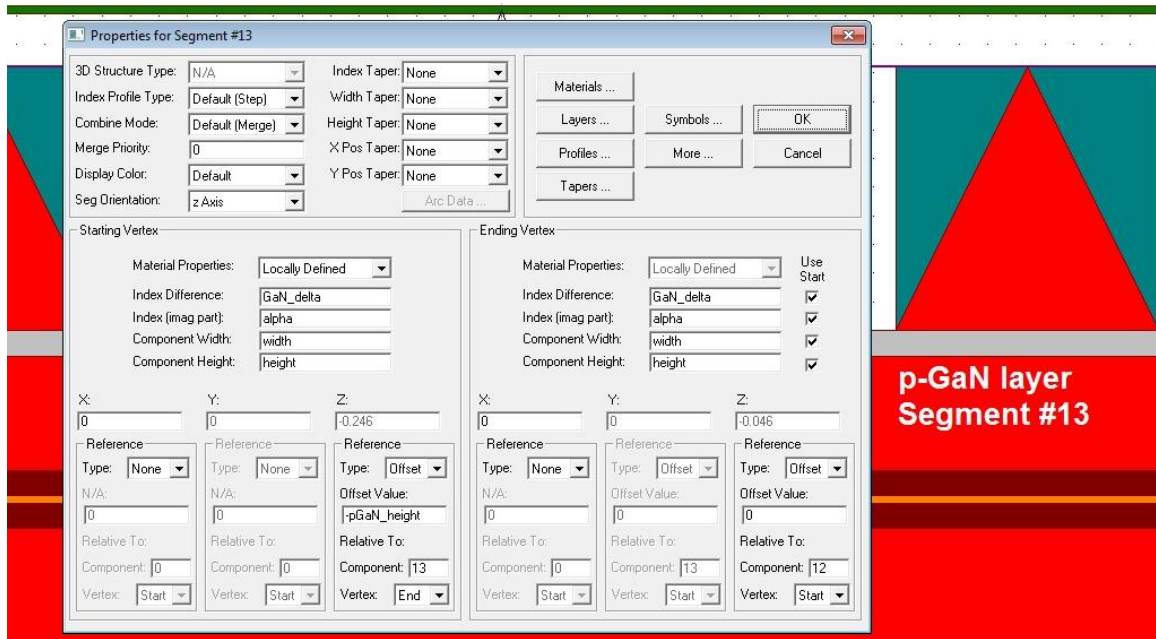


Figure 36 Adding the p-GaN layer.

Once the model is built, position the light emission bar in the middle of the MQW region add the light monitoring bars to the CAD space.

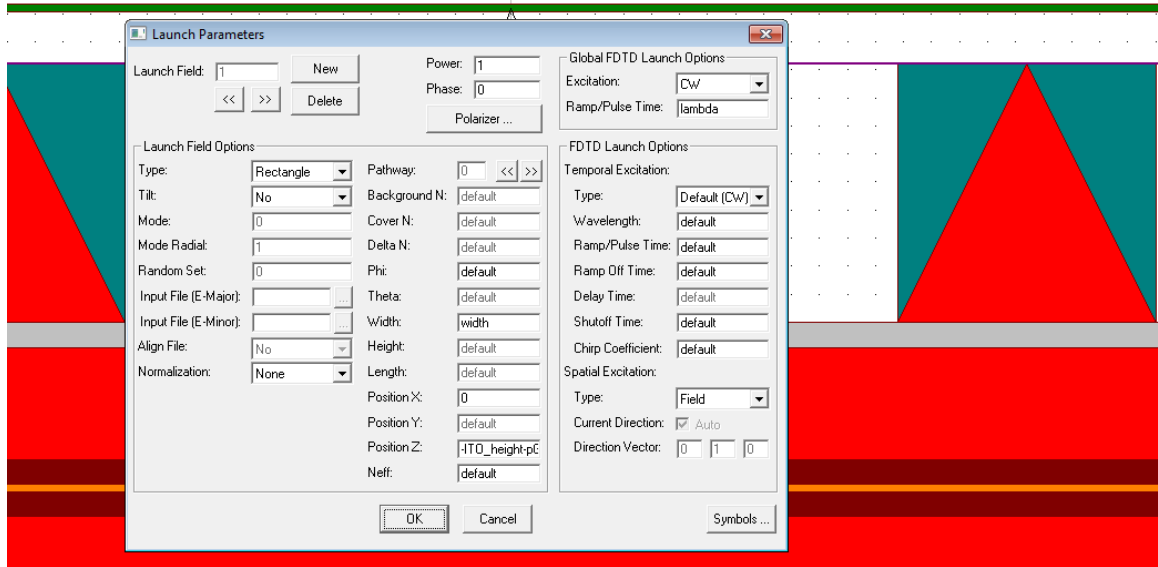


Figure 37 Light bar launch parameters.

The launch field specifies a continuous wave (CW) excitation that will mimic an LEDs light emission and allow for steady state conditions to be reached after running the simulation for a long enough time. Positioning the launch field bar in the middle of the MQW for an LED model that may have thicknesses change during the study requires that symbols be used to define the Z position of the bar. In Figure 37, Position Z is defined as '-ITO_height-pGaN_height-.5*MQW_height'.

After defining the launch field parameters, add the light field monitors to the CAD space. In Figure 38, the top light monitor, note that the Z position is fixed at $0.1\mu\text{m}$ above 0.46 , the maximum grating height. This position is held throughout all of the grating models to keep the distance between the non-grating portion of the LED and the light monitor constant. Also, time average is used on all light monitors to force a positive light output. If time averaging is turned off, the output intensity is shown as a high frequency sinusoid as the electromagnetic field changes from positive to negative. Since

we are interested in the intensity of the light output and not the phase of the light, time averaging was used on all monitors.

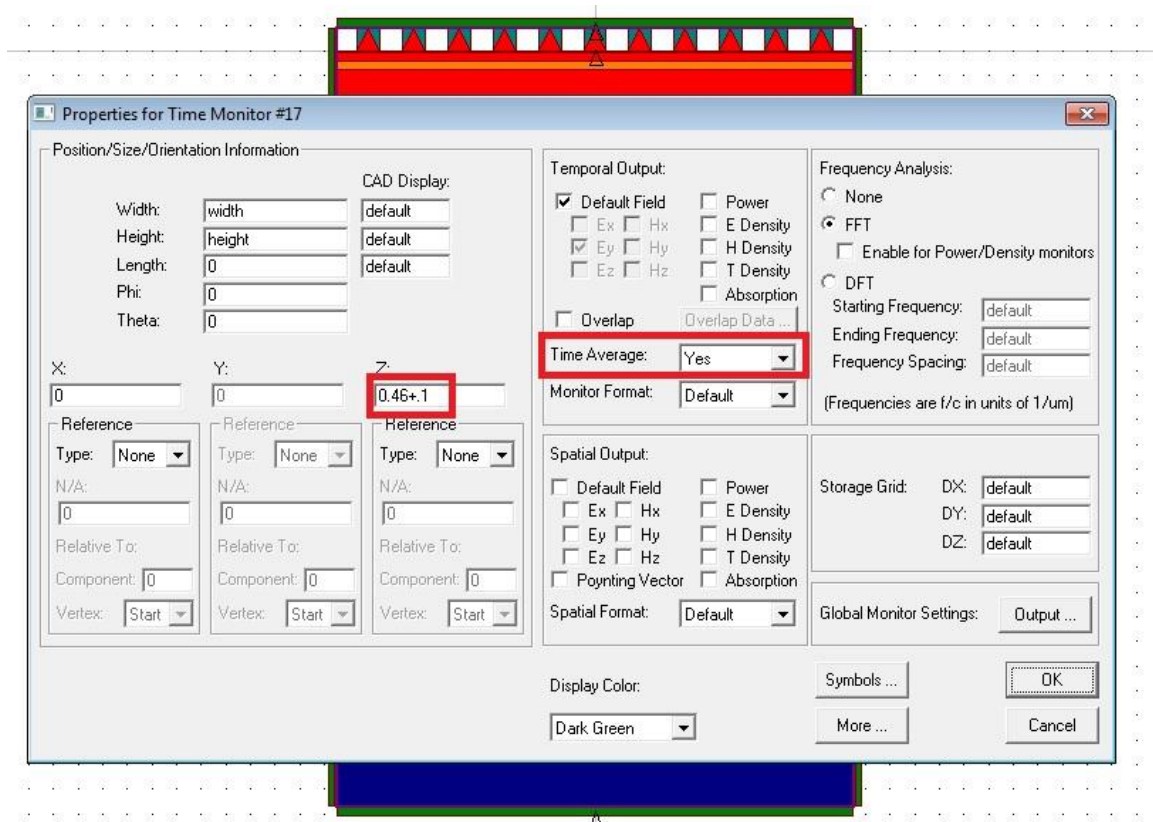


Figure 38 The top light monitor.

Setting up the left light monitor in Figure 39 is less intuitive than placing the top monitor and requires more thought. To make the monitor bar cover the entire left side, a symbol called 'total_height' is used. It is the sum of all material thicknesses plus the $0.47\mu\text{m}$ of grating space. By completely surrounding the LED with light monitors, we are able to record all light emitted from the LED and form an accurate picture of light distribution emerging from the device. Placing the light monitor at the correct height required the Z coordinate to be ' $-(\text{total_height})/2+.46$ '.

Follow the same steps for implementing monitors on the right side and the bottom of the LED.

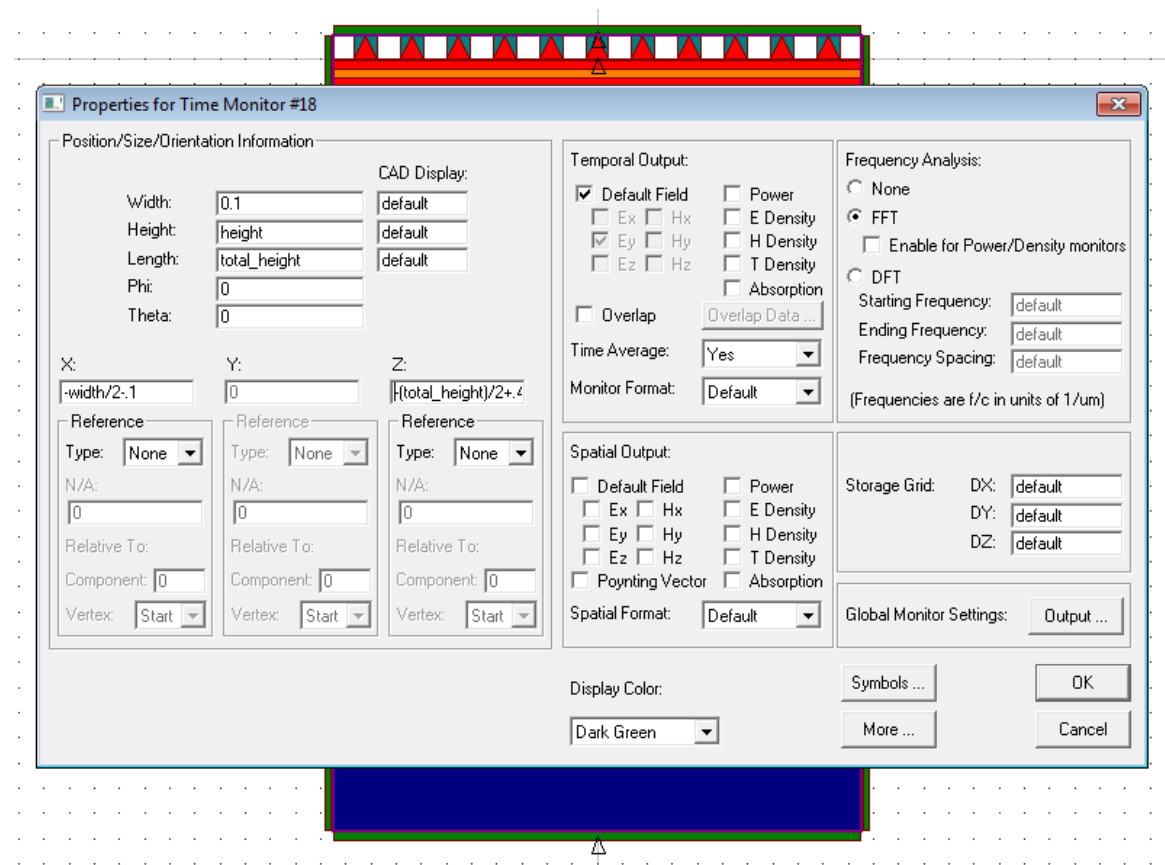


Figure 39 Left light monitor.

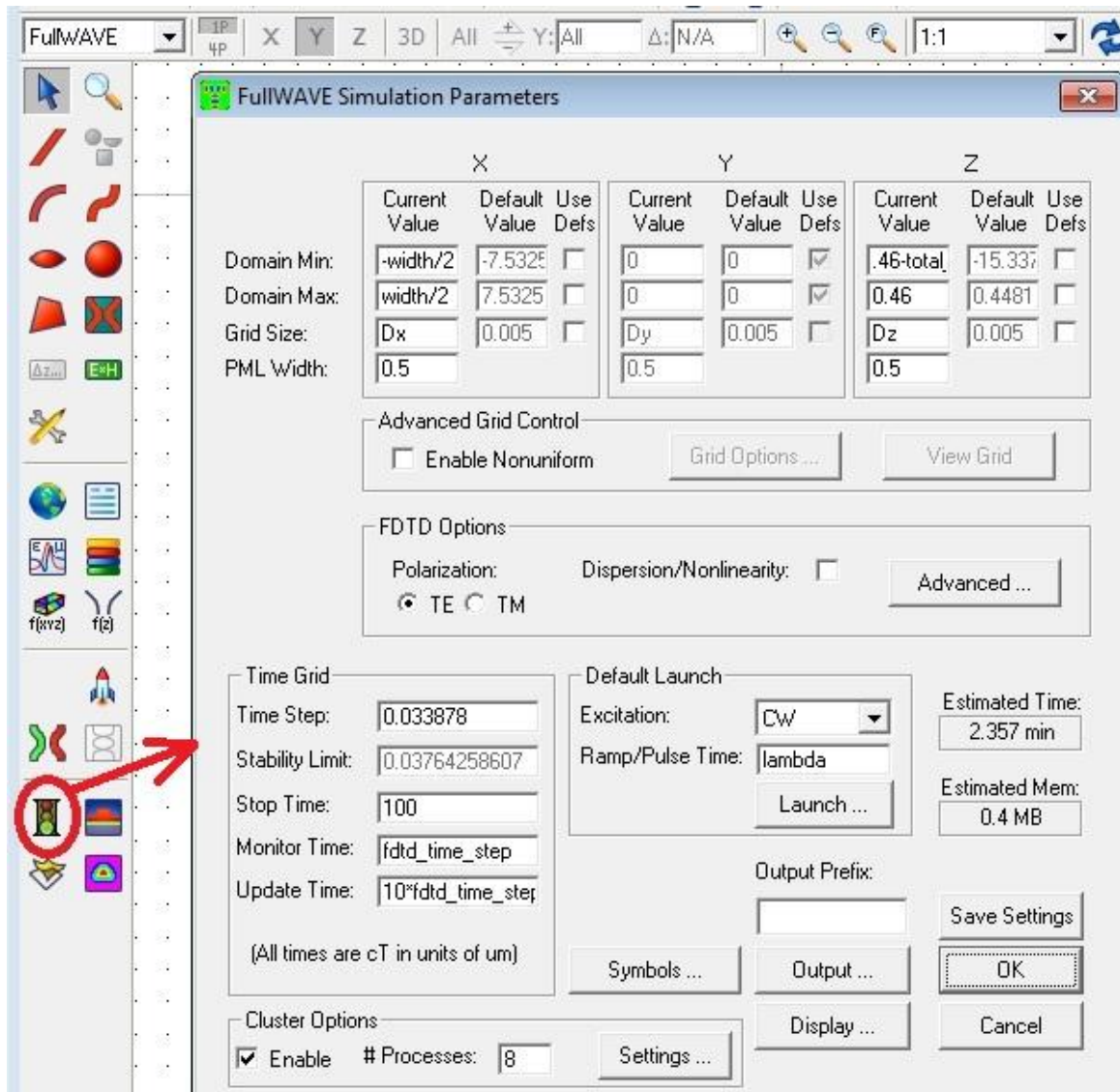


Figure 40 Setting up the simulation time steps and meshing.

After the model is built, select the stop light symbol to open the simulation parameters page. Before running a simulation, the parameters must be correctly set up to guarantee accurate results. Under grid size, each parameter must be less than 1/10 of a wavelength of the light being analyzed. If you chose to leave the default Dx and Dz like the example shows, back calculate what this value is by looking at its dependencies in the symbols window. Otherwise, make each components grid size equal to or smaller than a tenth of a wavelength. The 1/10th of a wavelength provides quicker results, but

decreasing the grid size below this minimum value increases simulation accuracy. Once grid sizes are chosen, RSoft will calculate the minimum time step limit for simulation stability, the value you chose must be smaller than the limit for the calculation to run correctly. Under cluster options the number of processes selected equals the number of CPU cores that the software will use - up to the maximum number of cores on your CPU. While this speeds up simulation time to some extent, its main benefit is reducing the amount of memory required for the simulation. The decrease in simulation time is barely noticeable.

Once a full grating model is done, building all future models can be completed much faster by using copy and paste, first using the text file and then within the CAD window. For the text file, copy all material definitions and boundary conditions (green font).

Grating Code 2

```
A = Period
Ax = A*sin(PhiPattern+PhiA)
Ay = 0
Az = A*cos(PhiPattern+PhiA)
B = A
Bx = 0
By = 1
Bz = 0
C = A
CellVolume = abs(Ax*(By*Cz-Bz*Cy)+Ay*(Bz*Cx-Bx*Cz)+Az*(Bx*Cy-By*Cx))
Cx = C*sin(PhiPattern+PhiC)
Cy = 0
Cz = C*cos(PhiPattern+PhiC)
DomainX = PeriodX
DomainZ = 2*PeriodZ
Dt = grid_size/2
Dx = PeriodX/16
Dy = 0.1
Dz = Dx*PeriodZ/PeriodX
GaN_delta = 2.5-background_index
ITO_height = 0.046
MQW_delta = 2.6-background_index
MQW_height = 0.1
NX = 11
NZ = 1
```

```

OffsetX = 0*Period
OffsetY = 0*Period
OffsetZ = 0*Period
Period = 0.92
PeriodX = Ax
PeriodZ = Cz
PhiA = 90
PhiC = 30
PhiCell = 0
PhiPattern = 0
Xmax = (NX+1)/2*PeriodX
Xmin = -Xmax
Zmax = (NZ+1)/2*PeriodZ
Zmin = -Zmax
alpha = 0
background_index = 1
boundary_max = width/2
boundary_min = -width/2
cad_aspectratio = 1
color_outline = 0
delta = 2.1-background_index
domain_max = 0.46
domain_min = .46-total_height
fdtd_monitor_time = fdtd_time_step
fdtd_mpi_enable = 1
fdtd_p0_index = 0
fdtd_ramp_time = lambda
fdtd_simmemcheck_warning = 0
fdtd_stop_time = 100
fdtd_time_step = 0.033878
fdtd_update_time = 10*fdtd_time_step
free_space_wavelength = 0.46
grid_size = Dx
grid_size_y = Dy
height = 0
index_display_mode = DISPLAY_CONTOURMAPXZ
lambda = free_space_wavelength
launch_position = 0
launch_position_z = -ITO_height-pGaN_height-.5*MQW_height
launch_type = LAUNCH_RECTANGLE
launch_width = width
nGaN_height = 5
pGaN_height = 0.2
pbg_layout = PBG_LAYOUT_HEX_XZ
profile_type = PROF_STEPINDEX
sapphire_delta = 1.77-background_index
sapphire_height = 10
sim_tool = ST_FULLWAVE
slice_grid_size = Dx
slice_grid_size_y = Dy
slice_step_size = Dz
step_size = Dz
total_height =
sapphire_height+nGaN_height+MQW_height+pGaN_height+ITO_height+.46
width = 10.5

```

```

*the grating references
circuit_reference 1
    profile_type =
PROF_INACTIVE
    color = 3
    reference_angle = PhiCell
    begin.x = -
5*Ax+0*Cx+OffsetX
    begin.y = OffsetY
    begin.z = -
5*Az+0*Cz+OffsetZ
    indfile = Cone-
2D(460sub000nm-460nm)T2.ind
end circuit_reference

```

```

circuit_reference 2
    profile_type =
PROF_INACTIVE
    color = 3
    reference_angle = PhiCell
    begin.x = -
4*Ax+0*Cx+OffsetX
    begin.y = OffsetY
    begin.z = -
4*Az+0*Cz+OffsetZ
    indfile = Cone-
2D(460sub000nm-460nm)T2.ind
end circuit_reference

```

```

circuit_reference 3
    profile_type =
PROF_INACTIVE
    color = 3
    reference_angle = PhiCell
    begin.x = -
3*Ax+0*Cx+OffsetX
    begin.y = OffsetY
    begin.z = -
3*Az+0*Cz+OffsetZ
    indfile = Cone-
2D(460sub000nm-460nm)T2.ind
end circuit_reference

```

```

circuit_reference 4
    profile_type =
PROF_INACTIVE
    color = 3
    reference_angle = PhiCell
    begin.x = -
2*Ax+0*Cx+OffsetX
    begin.y = OffsetY
    begin.z = -
2*Az+0*Cz+OffsetZ
    indfile = Cone-
2D(460sub000nm-460nm)T2.ind
end circuit_reference

```

```

circuit_reference 5
    profile_type =
PROF_INACTIVE
    color = 3
    reference_angle = PhiCell
    begin.x = -
1*Ax+0*Cx+OffsetX
    begin.y = OffsetY
    begin.z = -
1*Az+0*Cz+OffsetZ
    indfile = Cone-
2D(460sub000nm-460nm)T2.ind
end circuit_reference

```

```

circuit_reference 6
    profile_type =
PROF_INACTIVE
    color = 3
    reference_angle = PhiCell
    begin.x =
0*Ax+0*Cx+OffsetX
    begin.y = OffsetY
    begin.z =
0*Az+0*Cz+OffsetZ
    indfile = Cone-
2D(460sub000nm-460nm)T2.ind
end circuit_reference

```

```

circuit_reference 7
    profile_type =
PROF_INACTIVE
    color = 3
    reference_angle = PhiCell
    begin.x =
1*Ax+0*Cx+OffsetX
    begin.y = OffsetY
    begin.z =
1*Az+0*Cz+OffsetZ
    indfile = Cone-
2D(460sub000nm-460nm)T2.ind
end circuit_reference

```

```

circuit_reference 8
    profile_type =
PROF_INACTIVE
    color = 3
    reference_angle = PhiCell
    begin.x =
2*Ax+0*Cx+OffsetX
    begin.y = OffsetY
    begin.z =
2*Az+0*Cz+OffsetZ
    indfile = Cone-
2D(460sub000nm-460nm)T2.ind
end circuit_reference

```

```

circuit_reference 9
    profile_type =
PROF_INACTIVE
    color = 3
    reference_angle = PhiCell
    begin.x =
3*Ax+0*Cx+OffsetX
    begin.y = OffsetY
    begin.z =
3*Az+0*Cz+OffsetZ
    indfile = Cone-
2D(460sub000nm-460nm)T2.ind
end circuit_reference

circuit_reference 10
    profile_type =
PROF_INACTIVE
    color = 3
    reference_angle = PhiCell
    begin.x =
4*Ax+0*Cx+OffsetX

    begin.y = OffsetY
    begin.z =
5*Az+0*Cz+OffsetZ
    indfile = Cone-
2D(460sub000nm-460nm)T2.ind
end circuit_reference

circuit_reference 11
    profile_type =
PROF_INACTIVE
    color = 3
    reference_angle = PhiCell
    begin.x =
5*Ax+0*Cx+OffsetX
    begin.y = OffsetY
    begin.z =
5*Az+0*Cz+OffsetZ
    indfile = Cone-
2D(460sub000nm-460nm)T2.ind
end circuit_reference

```

*the LED material segments below can only be copy and pasted if the number of *grating segments used is the same for both files

```

segment 12
    color = 7
    begin.x = 0
    begin.z = -ITO_height rel end segment 12
    end.x = 0
    end.y = 0 rel begin segment 12
    end.z = 0
end segment

```

```

segment 13
    begin.x = 0
    begin.z = -pGaN_height rel end segment 13
    begin.delta = GaN_delta
    end.x = 0
    end.y = 0 rel begin segment 13
    end.z = 0 rel begin segment 12
    end.delta = GaN_delta
end segment

```

```

segment 14
    color = 4
    begin.x = 0
    begin.z = -MQW_height rel end segment 14
    begin.delta = MQW_delta
    end.x = 0
    end.y = 0 rel begin segment 14
    end.z = 0 rel begin segment 13
    end.delta = MQW_delta
end segment

```

```

segment 15
    begin.x = 0
    begin.z = -nGaN_height rel end segment 15

```



```

        begin.delta = GaN_delta
        end.x = 0
        end.y = 0 rel begin segment 15
        end.z = 0 rel begin segment 14
        end.delta = GaN_delta
end segment

segment 16
    color = 1
    begin.x = 0
    begin.z = -sapphire_height rel end segment 16
    begin.delta = sapphire_delta
    end.x = 0
    end.y = 0 rel begin segment 16
    end.z = 0 rel begin segment 15
    end.delta = sapphire_delta
end segment

time_monitor 17
    profile_type = PROF_INACTIVE
    color = 2
    type = TIMEMON_FIELD
    timeaverage = 1
    begin.x = 0
    begin.z = 0.46+.1
end time_monitor

time_monitor 18
    profile_type = PROF_INACTIVE
    color = 2
    type = TIMEMON_EXTENDED
    timeaverage = 1
    length = total_height
    begin.x = -width/2-.1
    begin.z = -(total_height)/2+.46
    begin.width = 0.1
end time_monitor

time_monitor 19
    profile_type = PROF_INACTIVE
    color = 2
    type = TIMEMON_EXTENDED
    timeaverage = 1
    length = total_height
    begin.x = width/2+.1
    begin.z = -(total_height)/2+.46
    begin.width = 0.1
end time_monitor

time_monitor 20
    profile_type = PROF_INACTIVE
    color = 2
    type = TIMEMON_FIELD
    timeaverage = 1
    begin.x = 0
    begin.z = -total_height-.1+.46
end time_monitor

```

Once the file has been updated to contain the symbols, open up the old and new files side by side as sub windows within the same RSoft CAD window. You can then copy and paste LED material segments from the old model into the new one. The copied material layers will go in the same physical locations that they were in for the old model, however, you must go into each segment and set it to be offset from the previous material layer so any change in material thickness will shift the whole model up or down. Otherwise material layer overlapping will occur.